International Journal of Systematic and Evolutionary Microbiology

Polyphasic data support the splitting of Aspergillus candidus into two species; proposal of A. dobrogensis sp. nov.

--Manuscript Draft--

Manuscript Number:	IJSEM-D-17-00864R1
Full Title:	Polyphasic data support the splitting of Aspergillus candidus into two species; proposal of A. dobrogensis sp. nov.
Article Type:	Taxonomic Description
Section/Category:	New taxa - Eukaryotic micro-organisms
Keywords:	antifungal susceptibility testing; antioxidant compounds; bioprospecting; cave mycobiota; indoor fungi; multispecies coalescence model
Corresponding Author:	Vit Hubka Charles University CZECH REPUBLIC
First Author:	Vit Hubka
Order of Authors:	Vit Hubka
	Alena Nováková
	Željko Jurjević
	František Sklenář
	Jens C. Frisvad
	Jos Houbraken
	Maiken C. Arendrup
	Karin M. Jørgensen
	João P.Z. Siqueira
	Josepa Gené
	Miroslav Kolařík
Manuscript Region of Origin:	CZECH REPUBLIC
Abstract:	Aspergillus candidus is a species frequently isolated from stored grain, food, indoor environment, soil and occasionally also from clinical material. Recent bioprospecting studies highlighted the potential of using A. candidus and its relatives in various industrial sectors as a result of their significant production of enzymes and bioactive compounds. A high genetic variability was observed among A. candidus isolates originating from various European countries and the USA, that were mostly isolated from indoor environments, caves and clinical material. The A. candidus sensu lato isolates were characterized by DNA sequencing of four genetic loci, and agreement between molecular species delimitation results, morphological characters and exometabolite spectra were studied. Classical phylogenetic methods (Maximum likelihood, Bayesian inference) and species delimitation methods based on the multispecies coalescent model supported recognition of up to three species in A. candidus sensu lato. After evaluation of phenotypic data, a broader species concept was adopted, and only one new species, A. dobrogensis, was proposed. This species is represented by 22 strains originating from seven countries (ex-type strain CCF 4651T = NRRL 62821T = IBT 32697T = CBS 143370T) and its differentiation from A. candidus is relevant for bioprospecting studies because these species produce different exometabolite profiles. Evaluation of the antifungal susceptibility of sect. Candidi members to six antifungals using the reference EUCAST method showed that all species have low minimum inhibitory concentrations for all tested antifungals. These results suggest applicability of a wide spectrum of antifungal agents for treatment of infections caused by species from sect. Candidi.

Polyphasic data support the splitting of *Aspergillus candidus* into two species; proposal of *A. dobrogensis* sp. nov.

Running title: Splitting of *Aspergillus candidus*

Vit Hubka[1,2*], Alena Nováková[2], Željko Jurjević[3], František Sklenář[1,2], Jens C. Frisvad[4], Jos Houbraken[5], Maiken C. Arendrup[6], Karin M. Jørgensen[6], João P. Z. Siqueira[7,8], Josepa Gené[8] and Miroslav Kolařík[1,2]

[1] Department of Botany, Faculty of Science, Charles University, Prague, Czech Republic
[2] Laboratory of Fungal Genetics and Metabolism, Institute of Microbiology of the Czech Academy of Sciences, Prague, Czech Republic
[3] EMSL Analytical, Inc., Cinnaminson, New Jersey, USA
[4] Department of Biotechnology and Biomedicine, Technical University of Denmark, Kongens Lyngby, Denmark
[5] Westerdijk Fungal Biodiversity Institute, Utrecht, The Netherlands
[6] Unit of Mycology, Department of Microbiology & Infection Control, Statens Serum Institut, Artillerivej 5, DK-2300, Copenhagen, Denmark
[7]Laboratório de Microbiologia, Faculdade de Medicina de São José do Rio Preto, 5416 Brigadeiro Faria Lima Ave., 15090-000, São José do Rio Preto, Brazil
[8]Unitat de Micologia, Facultat de Medicina i Ciències de la Salut, IISPV, Universitat Rovira i Virgili, Reus, Spain

*****corresponding authors e-mail: hubka@biomed.cas.cz; phone: +420 739663218

Key words: antifungal susceptibility testing, antioxidant compounds, bioprospecting, cave mycobiota, indoor fungi, multispecies coalescence model

contents category: new taxa (Eukaryotic micro-organisms)

The GenBank/ENA/DDBJ accession numbers for the ITS rDNA, β-tubulin, calmodulin and DNA-dependent RNA polymerase II, second largest subunit sequences of the ex-type strain CCF 4651^T of *Aspergillus dobrogensis* are LT626959, LT627027, LT558722 and LT627028, respectively.

The MycoBank (http://www.mycobank.org) accession number for *Aspergillus dobrogensis* is MB821313.

Abbreviations: *benA*, fragment of the β-tubulin gene; BI, Bayesian Inference; *CaM*, fragment of the calmodulin gene; EUCAST, European Committee on Antimicrobial Susceptibility testing; GM, geometric mean; ITS, fragment containing ITS1, 5.8S rDNA and ITS2 region of rDNA; MIC, minimum inhibitory concentration; ML, Maximum Likelihood; MSC, multispecies coalescent model; *RPB2*, fragment of the DNA-dependent RNA polymerase II, second largest subunit.

Abstract

Aspergillus candidus is a species frequently isolated from stored grain, food, indoor environment, soil and occasionally also from clinical material. Recent bioprospecting studies highlighted the potential of using *A. candidus* and its relatives in various industrial sectors as a result of their significant production of enzymes and bioactive compounds. A high genetic variability was observed among *A. candidus* isolates originating from various European countries and the USA, that were mostly isolated from indoor environments, caves and clinical material. The *A. candidus sensu lato* isolates were characterized by DNA sequencing of four genetic loci, and agreement between molecular species delimitation results, morphological characters and exometabolite spectra were studied. Classical phylogenetic methods (Maximum likelihood, Bayesian inference) and species delimitation methods based on the multispecies coalescent model supported recognition of up to three species in *A. candidus sensu lato*. After evaluation of phenotypic data, a broader species concept was adopted, and only one new species, *A. dobrogensis*, was proposed. This species is represented by 22 strains originating from seven countries (ex-type strain CCF 4651^{T} = NRRL 62821^{T} = IBT 32697^{T} = CBS 143370^{T}) and its differentiation from *A. candidus* is relevant for bioprospecting studies because these species produce different exometabolite profiles. Evaluation of the antifungal susceptibility of sect. *Candidi* members to six antifungals using the reference EUCAST method showed that all species have low minimum inhibitory concentrations for all tested antifungals. These results suggest applicability of a wide spectrum of antifungal agents for treatment of infections caused by species from sect. *Candidi*.

Introduction

Aspergillus section *Candidi* [1] currently encompasses six white- or yellow-sporulating species [2-4]. Apart from their morphology, which is broadly uniform across the majority of species, the taxonomy of the section is based on the physiology, exometabolite profiles and molecular data [2, 3]. *Aspergillus candidus* is the best known member of sect. *Candidi*. It is a xerophile and commonly found on stored grain, where it can decrease the grains' germinability. It is also frequently encountered in the indoor environment, on stored food and feedstuff (seeds, spices, grain products, nuts, dried products) and in soil [5-10].

Aspergillus candidus produces many bioactive compounds including anti-oxidative [11-14], cytotoxic [15], antitumor [16] and antimicrobial [11, 17, 18]. The species also has the potential to be used in biotechnology and waste degradation, as a result of its significant production of extracellular enzymes (e.g. acetamidase, inulinase, lipase, xylanase, etc.) [19-24] or in food manufacturing processes [25-28]. A variety of superficial and invasive infections have been attributed to *A. candidus* [29]; however, at least some of these cases were presumably caused by a related species *A. tritici* [2, 30, 31].

A considerable genetic variability was observed among *A. candidus* isolates during our previous studies on cave and indoor mycobiota and clinical fungi. In order to substantiate the initial finding, we assembled *A. candidus* strains isolated from various substrates in different European countries and the USA. We conducted DNA sequencing of four genetic loci, classical phylogenetic analysis, coalescence analysis, analysis of morphology and exometabolite spectra, and physiological testing in order to elucidate whether the detected level of genetic variability reflects undescribed species diversity or a high infraspecific variability.

Materials and Methods

Molecular studies. DNA was extracted from seven-day-old colonies with the ArchivePure DNA yeast and Gram2+ kit (5PRIME Inc., Gaithersburg, Maryland) using modifications described by Hubka *et al.* [32]. The ITS rDNA region was amplified using forward primers ITS1 and ITS5 [33] and reverse primers ITS4S [34] or NL4 [35]; partial *benA* gene encoding β-tubulin using forward primers Bt2a [36] or Ben2f [37] and reverse primer Bt2b [36]; partial *CaM* gene encoding calmodulin using forward primers CF1M or CF1L and reverse primer CF4 [38]; partial *RPB2* gene using forward primers fRPB2-5F [39] or RPB2-F50-CanAre [40] and reverse primer fRPB2-7cR [39]. The PCR protocol was described by Hubka *et al.* [2]. *RPB2* gene fragments were amplified using standard or touchdown thermal cycling [41].

PCR product purification followed the protocol described by Réblová *et al.* [42]. Automated sequencing was performed at Macrogen Sequencing Service (Amsterdam, The Netherlands) using the forward and reverse primers. Sequences were inspected and assembled using Bioedit v. 7.1.8 (www.mbio.ncsu.edu/BioEdit/bioedit.html). Obtained DNA sequences were deposited into the ENA (European Nucleotide Archive) database (Table 1).

Phylogenetic analysis. The ITS rDNA region was not used for phylogenetic analysis due to its low number of informative positions as recognized previously [2-4]. Alignments of the *benA*, *CaM* and *RPB2* regions were performed using the G-INS-i option implemented in [43]. Alignments were trimmed, concatenated and then analysed using Maximum Likelihood (ML) and Bayesian Inference (BI) analyses. The alignments is available from the Dryad Digital Repository: https://doi.org/10.5061/dryad.pg143.

A suitable partitioning scheme and substitution models (Bayesian information criterion) for analyses were selected using greedy strategy implemented in PartitionFinder v1.1.1 [44] with settings allowing introns, exons and codon positions to be independent partitions. The optimal partitioning scheme for ML analysis divided the dataset into five partitions with the following substitution models: K80+G substitution model was proposed for the *benA* and *CaM* introns; HKY+G model for the 3rd codon positions of *benA* and *CaM*; TrN+I model for 1st codon positions of *RPB2*, *benA* and *CaM*; HKY model for 2nd codon positions of *RPB2 benA* and *CaM*; and HKY+G model for the 3rd codon positions of *RPB2*. The ML tree was constructed with IQ-TREE version 1.4.4 [45] with nodal support determined by non-parametric bootstrapping (BS) with 1000 replicates. *Aspergillus petersonii* CCF 4999 was used as an outgroup.

Bayesian posterior probabilities (PP) were calculated using MrBayes 3.2.6 [46]. The optimal partitioning scheme and substitution models were selected as described above. The optimal partitioning scheme for BI analysis was similar to that for ML analysis except for the GTR+I model proposed for the 1st codon positions of *RPB2*, *benA* and *CaM*. The analyses ran for 10^7 generations, two parallel runs with four chains each were used, every 1000th tree was retained, and the first 25 % of trees were discarded as burn-in. Convergence was assessed by examining the likelihood plots in Tracer v. 1.6 [47].

Species delimitation using methods based on the multispecies coalescent model (MSC) and species tree inference. Three single-locus species delimitation methods, i.e., bGMYC [48], GMYC [49] and mPTP [50], and one multi locus species delimitation method STACEY [51] were used to find putative species boundaries within isolates identified as *A. candidus*. We followed Carstens *et al.* [52] and compared the results of several different methods. Three

genetic loci (*benA*, *CaM* and *RPB2*) were analyzed. Nucleotide substitution models for particular loci were determined using jModeltest v. 2.1.7 [53] based on Bayesian information criterion (BIC) and were as follows: K80 (*benA*), TrNef+I (*CaM*), TrN+I (*RPB2*).

Single locus ultrametric trees were constructed using a Bayesian approach in BEAST v. 2.4.5 [54] with both Yule and coalescent tree models. These trees were used as an input for the bGMYC and GMYC methods. Chain length for each tree was 1×10^7 generations with 25 % burn-in. The highest credibility tree was used for the GMYC method and 100 trees randomly sampled throughout the analysis were used for the bGMYC method. Both methods were performed in R 3.3.4 [55] using *bgmyc* [48] and *splits* (SPecies' LImits by Threshold Statistics) [49] packages. The non-ultrametric trees for the mPTP method were constructed using the ML approach in RAxML v. 7.7.1 [56] and IQ-TREE v. 1.5.3 [45] with 1000 bootstrap replicates. The mPTP programme was used with the following setting: Maximum likelihood species delimitation inference (option ML) and a different coalescent rate for each delimited species (option multi).

The multilocus species delimitation was performed in BEAST v. 2.4.5 with add-on STACEY v. 1.2.2 [51]. The chain length was set to 5×10^8 generations, priors were set as follows: the species tree prior was set to the Yule model, growth rate prior was set to lognormal distribution (M = 5, S = 2), clock rate priors for all loci were set to lognormal distribution (M = 0, S = 1), PopPriorScale prior was set to lognormal distribution (M = -7, S = 2) and relativeDeathRate prior was set to beta distribution ($\alpha = 1$, $\beta = 1000$). The output was processed with SpeciesDelimitationAnalyzer [51]. We also tested possible influence of strict and relaxed clock models on the results, but we did not find any differences.

The species tree was inferred using *BEAST [57] implemented in BEAST v. 2.4.5. For this analysis, only unique combined nucleotide sequences were selected with DAMBE v. 6.4.11 [58]. The isolates were assigned to a putative species according to the results of the above-mentioned species delimitation methods. The MCMC analysis ran for 1×10^8 generations, 25 % of trees were discarded as a burn-in. The strict molecular clock was chosen for all loci and population function was set as constant. Convergence was assessed by examining the likelihood plots in Tracer v. 1.6 [47]. We also constructed the tree with the same settings as above, but with each isolate defined as separate species.

The validation of the species hypotheses was performed in BP&P v. 3.3 (Bayesian phylogenetics and phylogeography) [59]. The isolates were assigned to the species based on the results of species delimitation methods and the species tree inferred with *BEAST was used as a guide tree. Three different combinations of the prior distributions of the parameters

θ (ancestral population size) and τ_0 (root age) were tested as proposed by Leaché and Fujita (2010), i.e., large ancestral population sizes and deep divergence: θ ~ G (1, 10) and τ_0 ~ G (1, 10); small ancestral population sizes and shallow divergences among species: θ ~ G (2, 2000) and τ_0 ~ G (2, 2000); large ancestral populations sizes and shallow divergences among species: θ ~ G (1, 10) and τ_0 ~ G (2, 2000).

R package *ggtree* [60] and the programme Densitree [61] were used for visualization of the phylogenetic trees.

Phenotypic studies and statistical analysis. For macormorphological characterization, the strains were grown on malt extract agar (MEA; malt extract from Oxoid Ltd., Basingstoke, UK), Czapek Yeast Extract Agar (CYA; yeast extract from Oxoid Ltd.), Czapek-Dox Agar (CZA) and Czapek Yeast Extract Agar with 20 % sucrose (CY20S). Agar media composition was based on that described by Samson *et al.* [62]. The production of acid compounds into the agar medium was tested on creatine sucrose agar (CREA). Growth at 30, 33, 35 and 37 °C was tested on MEA. Colour determination was performed according to the ISCC-NBS Centroid Colour Charts [63] (http://tx4.us/nbs-iscc.htm).

The micromorphology was observed on MEA after 10–14d of incubation at 25 °C as described by Hubka *et al.* [64]. Morphological characters were recorded at least 35 times for each isolate. Statistical differences in particular characters between species were tested with one-way ANOVA followed by Tukey´s HSD (honest significant difference) test in R v. 3.3.4 [55]. R package *multcomp* [65] was used for the calculation and package *ggplot2* [66] for visualization of the results.

Exometabolite analysis. The extracts were prepared according to Houbraken *et al.* [67]. Fungi were incubated for 1 week at 25 °C in darkness on CYA and yeast extract sucrose (YES) agars for exometabolite analysis. High-performance liquid chromatography with diode-array detection was performed according to Frisvad and Thrane [68, 69] as updated by Nielsen *et al.* [70].

Antifungal susceptibility testing. The determination of the minimum inhibitory concentrations (MICs) of antifungal agents was carried out according to the reference European Committee on Antimicrobial Susceptibility testing (EUCAST) guidelines (E.Def 9.3) for amphotericin B, terbinafine, itraconazole, posaconazole, voriconazole and isavuconazole [71]. Manufacturers and stock solutions (5000 mg L^{-1}) in DMSO (dimethyl sulfoxide; Sigma-Aldrich, Vallensbæk Strand, Denmark) were as follows: terbinafine (Novartis, Basel, Switzerland), posaconazole (Merck, Sharp and Dohme, Glostrup, Denmark), amphotericin B and itraconazole (Sigma-Aldrich, Brøndby, Denmark), isavuconazole

(Astellas Pharma Inc, Tokyo, Japan) and voriconazole (Pfizer A/S, Ballerup, Denmark). Plates were incubated at 30 °C to promote growth as suggested in EUCAST E.Def 7.2. *Candida parapsilosis* ATCC 22019 and *Candida krusei* ATCC 6258 were included as quality controls.

Results

Phylogenetic analysis

In the phylogenetic analysis, 54 combined *benA, CaM* and *RPB2* sequences were assessed for members of sect. *Candidi* (isolation source and accession numbers are listed in Table 1). The concatenated alignment contained 2133 characters, with 537 variable and 262 parsimony informative sites. In the best scoring Maximum likelihood tree shown in Fig. 1, members of sect. *Candidi* are resolved in several monophyletic clades or isolated single-strain lineages corresponding to six currently recognized species, namely *A. candidus, A. campestris, A. subalbidus, A. taichungensis, A. pragensis* and *A. tritici*. Twenty-one *Aspergillus* isolates originating from Romanian caves (n=11), indoor environment (n=6), clinical material (n=2) and mouse and herbivore dung (n=2) formed a highly supported monophyletic lineage (ML bootstrap support 91 % and BI posterior probability 0.99) sister to *A. candidus* s. str. These strains differed from *A. candidus* by phenotypic characters (see below) and are described below as *A. dobrogensis*.

The isolates of *A. dobrogensis* clustered into two highly supported clades, while several weakly supported clades were present in the *A. candidus* lineage (Fig. 1). Eleven of twenty *A. dobrogensis* isolates were recovered from the cave environment of three Romanian caves, where this species was most frequently found on bat guano (Fig. 2) and in the cave sediment. Further strains were obtained from indoor environment, clinical material and dung evidencing that *A. dobrogensis* is not exclusively a troglobitic species. Clade 1 of *A. dobrogensis* lineage (Fig. 1) contained only isolates from caves (n=9), while clade 2 (n=12) contained mostly isolates from the indoor environment (indoor air, carpet, dust, surface of a museum piece) and clinical material (human nails), but also two strains from caves and two strains from dung.

The ITS rDNA sequences of all investigated *A. dobrogensis* strains were identical to *A. candidus*, *A. subalbidus* and *A. pragensis*. The *benA* sequence of the ex-type strain of *A. dobrogensis* CCF 4651^{T} showed 95.3 % similarity to the ex-type of *A. candidus* NRRL 303^{T} (444/466 bp). The similarity of the *CaM* and *RPB2* sequences to *A. candidus* NRRL 303^{T} are 98.2 % (557/567 bp) and 98.6 % (1000/1014 bp), respectively. The infraspecific genetic varibility between *A. dobrogensis* strains was low making it easily distinguishable from *A.*

candidus by using *benA*, *CaM* and *RPB2* loci. There were seven variable sites in the *benA* alignment, eight in the *RPB2* alignment and only one in *CaM* alignment.

Species delimitation using MSC-based methods

Three genetic loci were examined across isolates identified as *A. candidus sensu lato*; and *A. tritici* lineage was also included in the analysis. Three tentative species (*A. tritici, A. candidus* and *A. dobrogensis*) were delimited in the analyzed dataset using the multi-locus delimitation method STACEY. The results are summarised in Fig. 3, and the differences in the colour of the tree branches reflect the proposed species delimitation.

Aspergillus tritici was consistently delimited from *A. candidus* and *A. dobrogensis* by all single-locus methods including their different settings (Fig. 3). Various delimitation schemes were proposed by different single-locus species delimitation methods in the *A. candidus*/*A. dobrogensis* lineages. The mPTP method based on all three loci and also bGMYC analysis based on the *RPB2* locus (only with input tree constructed using coalescent tree model) did not support delimitation of *A. dobrogensis* from *A. candidus*. In contrast, the results of bGMYC method based on the *benA* (input tree constructed using coalescent tree model), *CaM* and *RPB2* datasets (input tree constructed using Yule tree model) were in full agreement with the results of the STACEY analysis (Fig. 3). The GMYC method based on the *benA* and *RPB2* locus and also the bGMYC method based on *benA* locus (input tree constructed using Yule tree model) supported delimitation of an additional species within the *A. dobrogensis* lineage, corresponding to the two highly supported clades observed in the BI and ML analysis (Fig. 1). A significant over delimitation was observed in *A. candidus*/*A. dobrogensis* lineages when analyzing the *CaM* locus by GMYC method. The GMYC method also delimited several additional species in *A. candidus* lineage when analyzing *benA* and *RPB2* loci (Fig. 3). These putative species gained no support by any other analyses.

The species validation analysis results are appended to nodes of the tree in Fig. 3. Delimitation of all putative species proposed by STACEY were supported by the posterior probability 1.00 based on the analysis in BP&P v. 3.1 [59] under all three scenarios simulated by different prior distributions of parameters θ (ancestral population size) and τ_0 (root age).

The species tree topology was inferred with *BEAST [57] and is shown in Fig. 4. The analysis supported existence of up to four species that were highly supported (posterior probabilities = 1.00), i.e., *A. tritici*, *A. candidus* s. str. and two putative species in the *A. dobrogensis* lineage. There was no evidence of recombination between members of these lineages.

Phenotypic analysis

Growth parameters and macromorphological characters were assessed on four media and five temperatures. The results are summarized in Table 2. The colony morphology and growth parameters of *A. dobrogensis* are similar to those of *A. candidus*; however, on average, *A. dobrogensis* grows faster at 25 °C on all tested media (Table 2). The length and width of the stipe, and the diameter of vesicles significantly differed (Tukey´s HSD test, p value < 0.001) between *A. candidus* and *A. dobrogensis* (Fig. 5). The length of stipe was the most useful feature for differentiation of these species due to relatively lower overlap of values. The diameter of the conidia was identical for both species (Table 2, Fig. 5). No significant phenotypic differences were observed between isolates representing the two *A. dobrogensis* subclades (data not shown).

Exometabolites

There are chemotaxonomical differences between *A. candidus* and *A. dobrogensis* (Table 3). Barceloneic acid C, candidusins, terphenyllin and aspergilazine A are only found in some *A. candidus* isolates. A broad profile of aspergiloids [72] are found in *A. dobrogensis*, while only one aspergiloid is found in some strains of *A. candidus*. Brevianamide F seems to be a precursor of 12,13-dehydrodesoxybrevianamide E [= prolyl-2-(1',1'-dimethylallyl)tryptophyldiketopiperazine] and related compounds previously found in *A. pseudoustus* and *Pencillium italicum* [73-75]. They are found in both species, but *A. dobrogensis* produces a broader spectrum of these compounds. Similarly, the "Paspa" compounds are found in both species, but again *A. dobrogensis* produce a more broad profile of these compounds. These compounds may be equal to okaramins S-U [76], but this has yet to be confirmed. The uncharacterized compounds "ALKO", "MOYN", "MYO" and "TUT" are only found in *A. candidus*, while the "FMI" and the red compounds "AQ RED1" and "AQ RED2" are only found in *A. dobrogensis*. Retention indices and UV absorption maxima for the detected extrolites in *A. candidus* and *A. dobrogensis* are summarized in Table S1.

Antifungal susceptibility testing according the EUCAST method

The minimum inhibitory concentration (MIC) ranges and geometric mean (GM) values obtained by the EUCAST reference method for six antifungal agents (terbinafine, posaconazole, isavuconazole, voriconazole, itraconazole, amphotericin B) are shown in Table 4. Overall, all isolates across species in sect. *Candidi* were as susceptible as *A. fumigatus* to the

azoles and amphotericin B as MICs were below the EUCAST epidemiologic cut off values for these compounds against *A. fumigatus* (itraconazole: 1 mg/L, posaconazole: 0.25 mg/L, voriconazole: 1 mg/L, isavuconazole: 2 mg/L and amphotericin B: 1 mg/L) (Arendrup *et al.*, 2012; Arendrup *et al.*, 2016; Hope *et al.*, 2013). Exceptions were one isolates of *A. subalbidus* and one isolates of *A. taichungensis* for which the MIC of voriconazole was one dilution above the *A. fumigatus* ECOFF. Elevated MICs to terbinafine (4 mg L^{-1}) were recorded for two isolates of *A. candidus* and one isolate of *A. subalbidus*.

Description of *Aspergillus dobrogensis* A. Nováková, Ž. Jurjević, F. Sklenar, Frisvad, Houbraken & Hubka, sp. nov. (Figs. 2, 6)

Aspergillus dobrogensis (do.bro.gen´sis. N.L. masc. adj. *dobrogensis* pertaining to Dobrogea, Romania, the region of origin of the type specimen).

Description of micromorphology. *Conidial heads* on MEA white to cream white, radiate, biseriate, arising from aerial hyphae, rope-like structures occasionally present, coiling hyphae occasionally present. *Stipes* hyaline, smooth-walled, occasionally finely roughened, occasionally septate, (125–)150–2200(–3000) × (3.5–)4–13(–15) µm, diminutive conidiophores common, up to 100 long × 3–4(–5) µm diam; *vesicles* globose to subglobose, occasionally pyriform to elongate, (8–)9–31(–36) µm diam, diminutive vesicles 4–9 µm diam; *metulae* wedge-shaped (V-shaped) to cylindrical, (3–)4–17(–36) × (3–)4–10(–16) µm, covering the entire surface of vesicle; *phialides* ampuliform, (5–)6–9(–12) × 2.5–3.5(–4) µm, occasionally solitary phialides present up to 17 µm long. *Conidia* globose to subglobose, (3–)3.5–5(–5.5) µm (4 ± 0.3 µm), occasionally broadly ellipsoidal, smooth walled, occasionally finely roughened, larger spores borne on large phialides**.** *Sclerotia* purplish to black, occasionally cream to brown, sparse to abundant on MEA and CYA after 8 weeks.

Culture characteristics (at 25 °C after 2 wk). Colonies on MEA (21−)30−34(−37) mm diam (13−22 mm in 7 d), plane to delicately furrowed, zonate, delicately granular to granular, sporulation on whole surface or only in the colony centre with submerged margins, yellowish white (ISCC−NBS No. 92), no exudate, no soluble pigment, reverse colourless. Colonies on CYA (30−)38−42(−46) mm diam (18−26 mm in 7 d), plane to irregularly furrowed, with submerged margin, velutinous to delicately granular, sometimes floccose in colony centre, white (No. 263) to yellowish white (No. 92), no exudate to very small colourless droplets, no

soluble pigment, reverse colourless. Colonies on CZA (21−)24−28(−33) mm diam (12−17 mm in 7 d), plane, submerged lobate margins, zonate, delicately granular, yellowish white (No. 92), no exudate, no soluble pigment, reverse colourless. After 30 d the reverse is dark grey (No. 266) with occasional production of a dark grey soluble pigment. Colonies on CY20S (32−)35−38(−48) mm diam (20−27 mm in 7 d), plane with umbonate centre, floccose to delicately granular or granular, yellowish white (No. 92) to pale greyish yellow (No. 90) in colony centre, no exudate, no soluble pigment, reverse colourless to moderate yellow (No. 87). Growth parameters on MEA at 30 °C are comparable to 25 °C, no strains grew at 35 °C (Table 2).

The holotype specimen, PRM 935751, is deposited in the herbarium of the Mycological Department, National Museum, Prague, Czech Republic (PRM), and was isolated from cave sediment in the Movile Cave (Airbell II), Dobrogea region, Romania, collected and isolated by A. Nováková. The culture ex type is CCF 4651^{T} (= CCF 4655^{T} = NRRL 62821^{T} = IBT 32697^{T} = CBS 143370^{T}). The MycoBank deposit number is MB821313.

Morphological comparisons. *Aspergillus dobrogensis* differs from *A. candidus* by its longer and broader stipes and statistically significantly smaller vesicles (Table 2, Fig. 5). Almost all isolates of *A. dobrogensis* produced sclerotia on MEA and CYA, while the majority of *A. candidus* strains examined in this study did not produce sclerotia on CYA and none of the isolates produced them on MEA. In general, the average growth of *A. dobrogensis* isolates at 25 °C was more rapid on all tested media compared to *A. candidus* (Table 2). *Aspergillus campestris* can be differentiated by its sulfur yellow colonies; growth parameters of *A. pragensis* are slower on all media (especially CZA) and temperatures, and the colony reverse on MEA turns to red-brown after 2–3 weeks of cultivation; *A. subalbidus* grows also slightly slower than *A. dobrogensis* and has shorter stipes on MEA; *A. tritici* and *A. taichungensis* can be differentiated by their ability to grow at 37 °C.

Substrate and distribution. The species is known from bat droppings and guano, cave sediment, cave air, indoor air, dust, carpet, mouse dung, herbivore dung and clinical material; Czech Republic, Denmark, Germany, Romania, the Netherlands, Spain and the USA.

Discussion

A high degree of genetic variability among isolates of *A. candidus* was previously reported by Varga *et al.* [3], who preferred a broad species concept for *A. candidus*. As we demonstrated in this study, genetic diversity of *A. candidus sensu lato* strains is underlayed by both infraspecific variability and undescribed species diversity. The delimitation of a new species, *A. dobrogensis*, from *A. candidus* was supported by a polyphasic approach comprising multilocus sequence analyses, morphological and exometabolite data. Despite a relatively strong ecological clustering of the *A. dobrogensis* isolates into two clades with also high statistical phylogenetic support (Fig. 1), phenotypic or extrolite differences supporting the delimitation of two species in the *A. dobrogensis* lineage were not found. Due to this, we decided to introduce only one species, *A. dobrogensis*. In general, the ecology of *A. candidus* is very similar to *A. dobrogensis* and both species occur sympatrically on similar substrates (Fig. 1, Table 1).

Members of sect. *Candidi* are infrequently implicated in human infections. Although few in number, a wide spectrum of infections have been attributed to *A. candidus*, including invasive aspergillosis [77], lung abscess [78], meningitis [79], granuloma of the brain [80], sinusitis [81], otitis externa [2, 82-86] and onychomycosis [87-94]. Another member of sect. *Candidi*, *A. tritici*, is probably responsible for a part of reported infections attributed to *A. candidus* because it is able to grow at 37 °C in contrast to *A. candidus*. This species revived by Varga *et al.* [3] has been repeatedly detected in clinical samples when molecular methods were employed for species identification [30, 31, 95], and it has been confirmed as an agent of onychomycosis [30, 95]. In addition, some unrelated species can be misidentified as members of sect. *Candidi*. For instance, well-known causal agents of aspergillosis such as *A. fumigatus*, *A. flavus* and *A. terreus* occasionally produce white spored mutants [3, 96-98] and some naturally white spored species from sect. *Terrei* (*A. carneus* and *A. niveus*) are able to cause human infections as well [2, 99-102]. *Aspergillus pragensis*, a recently described member of sect. *Candidi* based on two isolates from clinical material in the Czech Republic, was isolated from indoor environment and outdoor air in the USA during this study (Fig. 1, Table 1) and was recently reported from Canadian house dust [10]. Clinical relevance of this species remains unconfirmed because both cases of suspected onychomycosis were not supported by repeated isolation of the species as required by guidelines for diagnosis of non-dermatophyte onychomycosis [103].

Previous studies reported a high *in vitro* activity of common antifungal agents against *A. candidus* [2, 104-106] and *A. tritici* [2, 31]. However, these studies usually included a limited number of isolates, used different methodologies for susceptibility testing and the characterization of strains was often based on phenotypic characters, resulting in unreliable

identifications. High MICs to amphotericin B detected in several isolates identified as *A. candidus* [105, 107] may indicate misidentification with species from sect. *Terrei* that are typical by intrinsic resistance to this antifungal [108]. In general, our results confirmed good *in vitro* activity of six antifungal agents against all members of sect. *Candidi* (Table 4). There was no clear antifungal susceptibility pattern typical for a particular species and overall the susceptibility pattern was similar to that for *A. fumigatus* [71, 109, 110].

Earlier studies on exometabolite production by members of sect. *Candidi* showed that these species produce unique compounds chlorflavonins, terphenyllin and candidusins, that are not present in other aspergilli [2, 3, 12, 111], except for *A. ellipticus* from sect. *Nigri* [112]. All these compounds have anti-oxidative properties, and they are most likely overproduced to protect the white/yellow conidia rather than via melanin, as opposed to species in closely related section *Nigri* that produce very large amounts of melanins [111].

Interestingly, antioxidant compounds candidusins, terphenyllin and its derivate 3-hydroxyterphenyllin were only detected in some strains of *A. candidus* while chlorflavonin was present in all examined strains of *A. candidus* and *A. dobrogensis* (Table 3). Thus, differentiation of these two species seems to be relevant especially for bioprospecting studies. For instance, antioxidant activity of some compounds and no production of mycotoxins make *A. candidus* suitable for the use in fermentation industry [28], and the extrolite 3-hydroxyterphenyllin has promising anticancer activity [16]. Similarly, barceloneic acid C, a compound with antibacterial activity [113] and aspergilazine A [114], which has antiviral activity, were detected only in *A. candidus* strains and not in *A. dobrogensis*. The production of many other uncharacterized compounds with unknown activity is in some cases species-specific (Table 3). It can be expected that both species also differ in extracellular enzymes production, some of which have industrial potential [19-24].

Funding Information

This research was supported by Czech Science Foundation (grant No. 17-20286S) and the project BIOCEV (CZ.1.05/1.1.00/02.0109) provided by the Ministry of Education, Youth and Sports of CR and ERDF. Vit Hubka is grateful for support from the Czechoslovak Microscopy Society (CSMS scholarship 2016).

Acknowledgements

We thank Milada Chudíčková and Birgit Brandt for her invaluable assistance in the laboratory, Stephen W. Peterson and P. Lysková for providing some isolates and the CCF

collection staff (Alena Kubátová - curator, Ivana Kelnarová and Adéla Kovaříčková) for deposition and lyophilization of the majority of cultures, and Veronica Jurjević for editing. Vit Hubka is grateful for support from Czechoslovak Microscopy Society (CSMS scholarship 2016).

Conflicts of Interest

The authors declare that that there is no conflict of interest.

References

1. Gams W, Christensen M, Onions AH, Pitt JI, Samson RA. Infrageneric taxa of *Aspergillus*. In: Samson RA, Pitt JI, editors. Advances in *Penicillium* and *Aspergillus* Systematics. New York: Plenum Press; 1985. p. 55–62.
2. Hubka V, Lyskova P, Frisvad JC, Peterson SW, Skorepova M, Kolarik M. *Aspergillus pragensis* sp. nov. discovered during molecular re-identification of clinical isolates belonging to *Aspergillus* section *Candidi*. Med Mycol. 2014;52:565–76.
3. Varga J, Frisvad JC, Samson RA. Polyphasic taxonomy of *Aspergillus* section *Candidi* based on molecular, morphological and physiological data. Stud Mycol. 2007;59:75–88.
4. Visagie CM, Hirooka Y, Tanney JB, Whitfield E, Mwange K, Meijer M, et al. *Aspergillus*, *Penicillium* and *Talaromyces* isolated from house dust samples collected around the world. Stud Mycol. 2014;78:63–139.
5. Klich MA. Biogeography of *Aspergillus* species in soil and litter. Mycologia. 2002;94(1):21–7.
6. Papavizas G, Christensen C. Grain storage studies. XXIX. Effect of invasion by individual species and mixtures of species of *Aspergillus* upon germination and development of discolored germs in wheat. Cereal Chem. 1960;37(2):197–203.
7. Pitt JI, Hocking AD. *Aspergillus* and related teleomorphs. In: Pitt JI, Hocking AD, editors. Fungi and food spoilage. London: Springer; 2009. p. 275-337.
8. Samson RA, Houbraken J, Thrane U, Frisvad JC, Andersen B. Food and indoor fungi. Utrecht: CBS KNAW Biodiversity Center; 2010. 269 p.
9. Sinha R, Wallace H. Storage stability of farm-stored rapeseed and barley. Can J Plant Sci. 1977;57(2):351–65.
10. Visagie CM, Yilmaz N, Renaud JB, Sumarah MW, Hubka V, Frisvad JC, et al. A survey of xerophilic *Aspergillus* from indoor environment, including descriptions of two new section *Aspergillus* species producing eurotium-like sexual states. MycoKeys. 2017;19:1–30.

11. Elaasser MM, Abdel-Aziz MM, El-Kassas RA. Antioxidant, antimicrobial, antiviral and antitumor activities of pyranone derivative obtained from *Aspergillus candidus*. Journal of Microbiology and Biotechnology Research. 2017;1(4):5–17.
12. Rahbæk L, Frisvad JC, Christophersen C. An amendment of *Aspergillus* section *Candidi* based on chemotaxonomical evidence. Phytochemistry. 2000;53(5):581–6.
13. Yen G-C, Chang Y-C, Sheu F, Chiang H-C. Isolation and characterization of antioxidant compounds from *Aspergillus candidus* broth filtrate. J Agric Food Chem. 2001;49(3):1426-31.
14. Yen G-C, Chiang H-C, Wu C-H, Yeh C-T. The protective effects of *Aspergillus candidus* metabolites against hydrogen peroxide-induced oxidative damage to Int 407 cells. Food Chem Toxicol. 2003;41(11):1561–7.
15. Takahashi C, Yoshihira K, Natori S, Umeda M. The structures of toxic metabolites of *Aspergillus candidus*. I. The compounds A and E, cytotoxic p-terphenyls. Chem Pharm Bull. 1976;24(4):613–20.
16. Wang Y, Compton C, Rankin GO, Cutler SJ, Rojanasakul Y, Tu Y, et al. 3-Hydroxyterphenyllin, a natural fungal metabolite, induces apoptosis and S phase arrest in human ovarian carcinoma cells. Int J Oncol. 2017;50(4):1392–402.
17. Shemshura ON, Bekmakhanova NE, Mazunina MN, Meyer SL, Rice CP, Masler EP. Isolation and identification of nematode-antagonistic compounds from the fungus *Aspergillus candidus*. FEMS Microbiol Lett. 2016;363(5):fnw026.
18. Wang R, Guo ZK, Li XM, Chen FX, Zhan XF, Shen MH. Spiculisporic acid analogues of the marine-derived fungus, *Aspergillus candidus* strain HDf2, and their antibacterial activity. Antonie Leeuwenhoek. 2015;108(1):215–9.
19. Farias CM, de Souza OC, Sousa MA, Cruz R, Magalhães OMC, de Medeiros ÉV, et al. High-level lipase production by *Aspergillus candidus* URM 5611 under solid state fermentation (SSF) using waste from *Siagrus coronata* (Martius) Becari. Afr J Biotechnol. 2015;14(9):820–8.
20. Garai D, Kumar V. Response surface optimization for xylanase with high volumetric productivity by indigenous alkali tolerant *Aspergillus candidus* under submerged cultivation. 3 Biotech. 2013;3(2):127–36.
21. Kochhar A, Gupta AK, Kaur N. Purification and immobilisation of inulinase from *Aspergillus candidus* for producing fructose. J Sci Food Agric. 1999;79(4):549–54.
22. Milala M, Shehu B, Zanna H, Omosioda V. Degradation of agro-waste by cellulase from *Aspergillus candidus*. Asian Journal of Biotechnology. 2009;1(2):51–6.

507 23. Rahim M, Saxena R, Gupta R, Sheoran A, Giri B. A novel and quick plate assay for
508 acetamidase producers and process optimization for its production by *Aspergillus candidus*.
509 Process Biochemistry. 2003;38(6):861–6.
510 24. Zheng P, Yu H, Sun Z, Ni Y, Zhang W, Fan Y, et al. Production of galacto-
511 oligosaccharides by immobilized recombinant β- galactosidase from *Aspergillus candidus*.
512 Biotechnol J. 2006;1(12):1464–70.
513 25. Grazia L, Romano P, Bagni A, Roggiani D, Guglielmi G. The role of moulds in the
514 ripening process of salami. Food Microbiol. 1986;3(1):19–25.
515 26. Spotti E, Mutti P, Scalari F. *Penicillium nalgiovense*, *P. gladioli*, *P. candidum* and
516 *Aspergillus candidus*. Possibility of their use as starter cultures. Industria Conserve.
517 1994;69:237–41.
518 27. Sunesen L, Stahnke L. Mould starter cultures for dry sausages—selection, application
519 and effects. Meat Sci. 2003;65(3):935–48.
520 28. Yen GC, Chang YC, Su SW. Antioxidant activity and active compounds of rice koji
521 fermented with *Aspergillus candidus*. Food Chem. 2003;83(1):49–54.
522 29. de Hoog GS, Guarro J, Gené J, Figueras MJ. Atlas of Clinical Fungi, 4th. ed. (USB-
523 version). Utrecht: CBS-KNAW Fungal Biodiversity Centre; 2014.
524 30. Hubka V, Kubatova A, Mallatova N, Sedlacek P, Melichar J, Skorepova M, et al. Rare
525 and new aetiological agents revealed among 178 clinical *Aspergillus* strains obtained from
526 Czech patients and characterised by molecular sequencing. Med Mycol. 2012;50:601–10.
527 31. Masih A, Singh PK, Kathuria S, Agarwal K, Meis JF, Chowdhary A. Clinically
528 significant rare *Aspergillus* species in a referral chest hospital, Delhi, India: molecular and
529 MALDI TOF identification and their antifungal susceptibility profiles. J Clin Microbiol.
530 2017:doi:10.1128/JCM.00962-16
531 32. Hubka V, Kolařík M, Kubátová A, Peterson SW. Taxonomical revision of *Eurotium*
532 and transfer of species to *Aspergillus*. Mycologia. 2013;105:912–37.
533 33. White TJ, Bruns T, Lee S, Taylor J. Amplification and direct sequencing of fungal
534 ribosomal RNA genes for phylogenetics. In: Innis MA, Gelfand DH, J. SJ, White TJ, editors.
535 PCR protocols: a guide to methods and applications. San Diego: Academic Press; 1990. p.
536 315–22.
537 34. Kretzer A, Li Y, Szaro T, Bruns TD. Internal transcribed spacer sequences from 38
538 recognized species of *Suillus* sensu lato: phylogenetic and taxonomic implications.
539 Mycologia. 1996;88(5):776–85.

35. O'Donnell K. *Fusarium* and its near relatives. In: Reynolds DR, Taylor JW, editors. The Fungal Holomorph: Mitotic, Meiotic and Pleomorphic Speciation in Fungal Systematics Wallingford: CAB International; 1993. p. 225–33.
36. Glass NL, Donaldson GC. Development of primer sets designed for use with the PCR to amplify conserved genes from filamentous ascomycetes. Appl Environ Microbiol. 1995;61(4):1323–30.
37. Hubka V, Kolařík M. β-tubulin paralogue *tubC* is frequently misidentified as the *benA* gene in *Aspergillus* section *Nigri* taxonomy: primer specificity testing and taxonomic consequences. Persoonia. 2012;29:1–10.
38. Peterson SW. Phylogenetic analysis of *Aspergillus* species using DNA sequences from four loci. Mycologia. 2008;100(2):205–26.
39. Liu YJ, Whelen S, Hall BD. Phylogenetic relationships among ascomycetes: evidence from an RNA polymerse II subunit. Mol Biol Evol. 1999;16(12):1799–808.
40. Jurjević Ž, Kubátová A, Kolařík M, Hubka V. Taxonomy of *Aspergillus* section *Petersonii* sect. nov. encompassing indoor and soil-borne species with predominant tropical distribution. Pl Syst Evol. 2015;301:2441–62.
41. Hubka V, Nováková A, Peterson SW, Frisvad JC, Sklenář F, Matsuzawa T, et al. A reappraisal of *Aspergillus* section *Nidulantes* with descriptions of two new sterigmatocystin producing species. Pl Syst Evol. 2016;302:1267–99.
42. Réblová M, Hubka V, Thureborn O, Lundberg J, Sallstedt T, Wedin M, et al. From the tunnels into the treetops: new lineages of black yeasts from biofilm in the Stockholm metro system and their relatives among ant-associated fungi in the *Chaetothyriales*. PLoS One. 2016;11(10):e0163396.
43. Katoh K, Standley DM. MAFFT multiple sequence alignment software version 7: improvements in performance and usability. Mol Biol Evol. 2013;30(4):772–80.
44. Lanfear R, Calcott B, Ho SY, Guindon S. PartitionFinder: combined selection of partitioning schemes and substitution models for phylogenetic analyses. Mol Biol Evol. 2012;29(6):1695–701.
45. Nguyen L-T, Schmidt HA, von Haeseler A, Minh BQ. IQ-TREE: A fast and effective stochastic algorithm for estimating maximum-likelihood phylogenies. Mol Biol Evol. 2015;32(1):268–74.
46. Ronquist F, Teslenko M, van der Mark P, Ayres DL, Darling A, Höhna S, et al. MrBayes 3.2: efficient Bayesian phylogenetic inference and model choice across a large model space. Syst Biol. 2012;61:539-42.

47. Rambaut A, Suchard M, Xie D, Drummond A. Tracer v1. 6. 2014, website http://beast.bio.ed.ac.uk 2014.
48. Reid NM, Carstens BC. Phylogenetic estimation error can decrease the accuracy of species delimitation: a Bayesian implementation of the general mixed Yule-coalescent model. BMC Evol Biol. 2012;12(1):196.
49. Fujisawa T, Barraclough TG. Delimiting species using single-locus data and the Generalized Mixed Yule Coalescent approach: a revised method and evaluation on simulated data sets. Syst Biol. 2013;62(5):707–24.
50. Kapli P, Lutteropp S, Zhang J, Kobert K, Pavlidis P, Stamatakis A, et al. Multi-rate Poisson tree processes for single-locus species delimitation under maximum likelihood and Markov chain Monte Carlo. Bioinformatics. 2017;33(11):1630–8.
51. Jones G. Algorithmic improvements to species delimitation and phylogeny estimation under the multispecies coalescent. J Math Biol. 2017;74(1-2):447–67.
52. Carstens BC, Pelletier TA, Reid NM, Satler JD. How to fail at species delimitation. Mol Ecol. 2013;22(17):4369–83.
53. Posada D. jModelTest: phylogenetic model averaging. Mol Biol Evol. 2008;25(7):1253–6.
54. Bouckaert R, Heled J, Kühnert D, Vaughan T, Wu C-H, Xie D, et al. BEAST 2: a software platform for Bayesian evolutionary analysis. PLoS Comput Biol. 2014;10(4):e1003537.
55. R_Core_Team. R: A language and environment for statistical computing. Vienna: R Foundation for Statistical Computing; 2015.
56. Stamatakis A, Hoover P, Rougemont J. A rapid bootstrap algorithm for the RAxML web servers. Syst Biol. 2008;57(5):758–71.
57. Heled J, Drummond AJ. Bayesian inference of species trees from multilocus data. Mol Biol Evol. 2010;27(3):570–80.
58. Xia X. DAMBE6: new tools for microbial genomics, phylogenetics, and molecular evolution. J Hered. 2017;108(4):431–7.
59. Yang Z, Rannala B. Bayesian species delimitation using multilocus sequence data. Proceedings of the National Academy of Sciences. 2010;107(20):9264–9.
60. Yu G, Smith DK, Zhu H, Guan Y, Lam TTY. ggtree: an R package for visualization and annotation of phylogenetic trees with their covariates and other associated data. Methods Ecol Evol. 2017;8(1):28–36.

607 61. Bouckaert RR. DensiTree: making sense of sets of phylogenetic trees. Bioinformatics.
608 2010;26(10):1372–3.
609 62. Samson RA, Visagie CM, Houbraken J, Hong SB, Hubka V, Klaassen CHV, et al.
610 Phylogeny, identification and nomenclature of the genus *Aspergillus*. Stud Mycol.
611 2014;78:141–73.
612 63. Kelly KL. Inter-society color council – National bureau of standards color name charts
613 illustrated with centroid colors. Washington: US Government Printing Office; 1964. 36 p.
614 64. Hubka V, Novakova A, Kolarik M, Jurjevic Z, Peterson SW. Revision of *Aspergillus*
615 section *Flavipedes*: seven new species and proposal of section *Jani* sect. nov. Mycologia.
616 2015;107(1):169–208.
617 65. Hothorn T, Bretz F, Westfall P. Simultaneous inference in general parametric models.
618 Biometrical Journal. 2008;50(3):346–63.
619 66. Wickham H. ggplot2: Elegant Graphics for Data Analysis. New York: Springer-
620 Verlag; 2009.
621 67. Houbraken J, Spierenburg H, Frisvad JC. *Rasamsonia*, a new genus comprising
622 thermotolerant and thermophilic *Talaromyces* and *Geosmithia* species. Antonie
623 Leeuwenhoek. 2012;101(2):403–21.
624 68. Frisvad JC, Thrane U. Standardized high-performance liquid chromatography of 182
625 mycotoxins and other fungal metabolites based on alkylphenone retention indices and UV-
626 VIS spectra (diode array detection). J Chromatogr A. 1987;404(1):195–214.
627 69. Frisvad JC, Thrane U. Liquid column chromatography of mycotoxins. In: Betina V,
628 editor. Chromatography of mycotoxins: techniques and applications Journal of
629 Chromatography Library 541993. p. 253–372.
630 70. Nielsen KF, Månsson M, Rank C, Frisvad JC, Larsen TO. Dereplication of microbial
631 natural products by LC-DAD-TOFMS. J Nat Prod. 2011;74(11):2338–48.
632 71. Arendrup MC, Meletiadis J, Mouton J, Guinea J, Cuenca-Estrella M, Lagrou K, et al.
633 EUCAST technical note on isavuconazole breakpoints for *Aspergillus*, itraconazole
634 breakpoints for *Candida* and updates for the antifungal susceptibility testing method
635 documents. Clin Microbiol Infect. 2016;22(6):571. e1-. e4.
636 72. Guo ZK, Yan T, Guo Y, Song YC, Jiao RH, Tan RX, et al. P-terphenyl and
637 diterpenoid metabolites from endophytic *Aspergillus* sp. YXf3. J Nat Prod. 2012;75(1):15–21.
638 73. Arai K, Miyajima H, Mushiroda T, Yamamoto Y. Metabolites of *Penicillium italicum*
639 Wehmer: isolation and structures of new metabolites including naturally occurring 4-ylidene-

640 acyltetronic acids, italicinic acid and italicic acid. Chemical and Pharmaceutical Bulletin.
641 1989;37(12):3229–35.
642 74. Steyn P. Austamide, a new toxic metabolite from *Aspergillus ustus*. Tetrahedron Lett.
643 1971;12(36):3331–4.
644 75. Steyn P. The structures of five diketopiperazines from *Aspergillus ustus*. Tetrahedron.
645 1973;29(1):107–20.
646 76. Cai S, Sun S, Peng J, Kong X, Zhou H, Zhu T, et al. Okaramines S–U, three new
647 indole diketopiperazine alkaloids from *Aspergillus taichungensis* ZHN-7-07. Tetrahedron.
648 2015;71(22):3715–9.
649 77. Iwasaki K, Tategami T, Sakamoto Y, Yasutake T, Otsubo S. An operated case report
650 of pulmonary aspergillosis by sapprophytic infection of Aspergillus candidus in congenital
651 bronchial cyst of right lower lobe. Kyobu geka The Japanese journal of thoracic surgery.
652 1991;44(5):429-32.
653 78. Becker A, Sifaoui F, Gagneux M, Desprez S, Vignoli P, Huguet D, et al. Drug
654 interactions between voriconazole, darunavir/ritonavir and tenofovir/emtricitabine in an HIV-
655 infected patient treated for *Aspergillus candidus* lung abscess. Int J STD AIDS.
656 2015;26(9):672–5.
657 79. Moling O, Lass- Floerl C, Verweij P, Porte M, Boiron P, Prugger M, et al. Chronic
658 and acute *Aspergillus* meningitis. Mycoses. 2002;45(11–12):504–11.
659 80. Linares G, McGarry PA, Baker RD. Solid solitary aspergillotic granuloma of the brain
660 Report of a case due to *Aspergillus candidu*s and review of the literature. Neurology.
661 1971;21(2):177–84.
662 81. Avanzini F, Bigoni A, Nicoletti G. A rare case of isolated aspergilloma of the
663 sphenoid sinus. Acta Otorhinolaryngol Ital. 1991;11(5):483–9.
664 82. Falser N. Mycotic infection of the ear. Harmless saprophyte or pathognomonic risk
665 factor? PILZBEFALL DES OHRES - HARMLOSER SAPROPHYT ODER
666 PATHOGNOMONISCHER RISIKOFAKTOR? 1983;62(4):140-6.
667 83. García-Agudo L, Aznar-Marín P, Galán-Sánchez F, García-Martos P, Marín-Casanova
668 P, Rodríguez-Iglesias M. Otomycosis due to filamentous fungi. Mycopathologia.
669 2011;172(4):307–10.
670 84. Vennewald I, Schönlebe J, Klemm E. Mycological and histological investigations in
671 humans with middle ear infections. Mycoses. 2003;46(1- 2):12-8.
672 85. Vennewald I, Schönlebe J, Klemm E. Histologic studies on otomycosis. Mycoses.
673 2002;45:47-52.

86. Yassin A, Maher A, Moawad M. Otomycosis: a survey in the eastern province of Saudi Arabia. J Laryngol Otol. 1978;92(10):869–76.
87. Ahmadi B, Hashemi SJ, Zaini F, Shidfar MR, Moazeni M, Mousavi B, et al. A case of onychomycosis caused by *Aspergillus candidus*. Med Mycol Case Rep. 2012;1(1):45–8.
88. Cornere B, Eastman M. Onychomycosis due to *Aspergillus candidus*: case report. N Z Med J. 1975;82(543):13–5.
89. Fragner P, Kubickova V. Onychomycosis due to *Aspergillus candidus*. Cesk Dermatol. 1974;49(5):322–4.
90. Gupta A, Gupta G, Jain H, Lynde C, Foley K, Daigle D, et al. The prevalence of unsuspected onychomycosis and its causative organisms in a multicentre Canadian sample of 30 000 patients visiting physicians' offices. J Eur Acad Dermatol Venereol. 2016;30(9):1567–72.
91. Kaben U. *Aspergillus candidus* Link as the cause of onychomycosis. Z Haut Geschlechtskr. 1962;32:50–3.
92. Nouripour-Sisakht S, Mirhendi H, Shidfar M, Ahmadi B, Rezaei-Matehkolaei A, Geramishoar M, et al. *Aspergillus* species as emerging causative agents of onychomycosis. J Mycol Med. 2015;25(2):101–7.
93. Piraccini BM, Tosti A. White superficial onychomycosis: epidemiological, clinical, and pathological study of 79 patients. Arch Dermatol. 2004;140(6):696–701.
94. Zaror L, Moreno M. Onychomycosis due to *Aspergillus candidus* Link. Rev Argent Micol. 1980;3(3):13–5.
95. Zotti M, Machetti M, Persi A, Barabino G, Mariotti M, Parodi A. Different species of *Aspergillus* involved in ungual pathologies. Journal of Biological Research-Bollettino della Società Italiana di Biologia Sperimentale. 2011;84(1):171–3.
96. Cole RJ, Hill RA, Blankenship PD, Sanders TH. Color mutants of *Aspergillus flavus* and *Aspergillus parasiticus* in a study of preharvest invasion of peanuts. Appl Environ Microbiol. 1986;52(5):1128–31.
97. Jackson JC, Higgins LA, Lin X. Conidiation color mutants of *Aspergillus fumigatus* are highly pathogenic to the heterologous insect host *Galleria mellonella*. PLoS One. 2009;4(1):e4224.
98. Raper KB, Fennell DI. The genus *Aspergillus*. Baltimore: Williams & Wilkins Co.; 1965. 686 p.

99. Auberger J, Lass-Flörl C, Clausen J, Bellmann R, Buzina W, Gastl G, et al. First case of breakthrough pulmonary *Aspergillus niveus* infection in a patient after allogeneic hematopoietic stem cell transplantation. Diagn Microbiol Infect Dis. 2008;62(3):336–9.
100. Morquer R, Enjalbert L. Sur un nouvel agent de l'aspergillose humaine. Rev Mycol Paris. 1957;22:130–54.
101. Morquer R, Enjalbert L. Étude morphologique et physiologique d'une *Aspergillus* nouvellement isolé au cors d'un affection pulmonaire de l'homme. C R Soc Biol Paris. 1957;244:1405–8.
102. Pore R, Larsh H. Experimental pathology of *Aspergillus terreus-flavipes* group species. Med Mycol. 1968;6(2):89–93.
103. Summerbell RC, Cooper E, Bun U, Jamieson F, Gupta AK. Onychomycosis: A critical study of techniques and criteria for confirming the etiologic significance of nondermatophytes. Med Mycol. 2005;43(1):39–59.
104. García-Martos P, García-Agudo L, Gutiérrez-Calzada J, Ruiz-Aragón J, Saldarreaga A, Marín P. In vitro activity of amphotericin B, itraconazole and voriconazole against 20 species of *Aspergillus* using the Sensititre® microdilution method. Enferm Infecc Microbiol Clin. 2005;23(1):15–8.
105. Gomez-Lopez A, Garcia-Effron G, Mellado E, Monzon A, Rodriguez-Tudela JL, Cuenca-Estrella M. In vitro activities of three licensed antifungal agents against Spanish clinical isolates of *Aspergillus* spp. Antimicrob Agents Chemother. 2003;47(10):3085–8.
106. Wildfeuer A, Seidl H, Paule I, Haberreiter A. *In vitro* evaluation of voriconazole against clinical isolates of yeasts, moulds and dermatophytes in comparison with itraconazole, ketoconazole, amphotericin B and griseofulvin. Mycoses. 1998;41(7- 8):309–19.
107. Dóczi I, Dósa E, Varga J, Antal Z, Kredics L, Nagy E. Etest for assessing the susceptibility of filamentous fungi. Acta Microbiol Immunol Hung. 2004;51(3):271–81.
108. Risslegger B, Zoran T, Lackner M, Aigner M, Sánchez-Reus F, Rezusta A, et al. A prospective international *Aspergillus terreus* survey: an EFISG, ISHAM and ECMM joint study. Clin Microbiol Infect. 2017:doi:10.1016/j.cmi.2017.04.012.
109. Arendrup MC, Cuenca- Estrella M, Lass- Flörl C, Hope W. EUCAST technical note on the EUCAST definitive document EDef 7.2: method for the determination of broth dilution minimum inhibitory concentrations of antifungal agents for yeasts EDef 7.2 (EUCAST-AFST). Clin Microbiol Infect. 2012;18(7):E246–E7.

738 110. Hope W, Cuenca- Estrella M, Lass- Flörl C, Arendrup M, (EUCAST-AFST)
739 TECoASTSoAST. EUCAST technical note on voriconazole and *Aspergillus* spp. Clin
740 Microbiol Infect. 2013;19(6):E278–E80.
741 111. Frisvad JC, Larsen TO. Chemodiversity in the genus *Aspergillus*. Appl Microbiol
742 Biotechnol. 2015;99(19):7859–77.
743 112. Samson RA, Noonim P, Meijer M, Houbraken J, Frisvad JC, Varga J. Diagnostic tools
744 to identify black aspergilli. Stud Mycol. 2007;59:129–45.
745 113. Xia X, Kim S, Bang S, Lee H-J, Liu C, Park C-I, et al. Barceloneic acid C, a new
746 polyketide from an endophytic fungus *Phoma* sp. JS752 and its antibacterial activities. J
747 Antibiot. 2015;68(2):139–41.
748 114. Cai S, Kong X, Wang W, Zhou H, Zhu T, Li D, et al. Aspergilazine A, a
749 diketopiperazine dimer with a rare N-1 to C-6 linkage, from a marine-derived fungus
750 *Aspergillus taichungensis*. Tetrahedron Lett. 2012;53(21):2615–7.

751

752 **Figure legends**

753 **Fig. 1.** Phylogenetic relationships of the sect. *Candidi* members inferred from Bayesian analysis
754 of the combined, 3-gene data set of β-tubulin (*benA*), calmodulin (*CaM*) and RNA polymerase
755 II second largest subunit (*RPB2*) genes. Bayesian posterior probability (PP) and Maximum
756 likelihood bootstrap support (BS) are appended to nodes; only PP ≥ 90 % and BS ≥ 70 % and
757 are shown; lower supports are indicated with a hyphen; ex-type strains are designated by a
758 superscript T. The tree is rooted with *Aspergillus petersonii* CCF 4999^{T}.

759

760 **Fig. 2.** Colonies of *Aspergillus dobrogensis* on bat guano in the Liliecilor de la Gura Dobrogei
761 Cave (a–b).

762

763 **Fig. 3.** Schematic representation of results of species delimitation methods in section *Candidi*
764 based on *benA*, *CaM* and *RPB2* sequence data. The results of multilocus method (STACEY)
765 are compared to results of single-locus methods. The results of STACEY are shown as tree
766 branches with different colours, while the results of single-locus methods (PTP, bGMYC,
767 GMYC) are depicted with coloured bars (different colours, including different colour shades,
768 indicate tentative species delimited by particular methods). The species validation analysis
769 results (BP&P) are appended to nodes and shown in gray bordered boxes; the values represent
770 posterior probabilities calculated in three scenarios [top value: $\theta \sim$ G (1, 10) and $\tau_0 \sim$ G (1,

771 10); middle value: θ ~ G (1, 10) and τ_0 ~ G (2, 2000); bottom value: θ ~ G (2, 2000) and τ_0 ~
772 G (2, 2000)]. The displayed maximum likelihood tree was inferred with IQ-TREE and based
773 on a concatenated alignment of *benA*, *CaM* and *RPB2* loci [1000 bootstrap replicates;
774 partitioning scheme was determined as described in Material and Methods], and is used solely
775 for the comprehensive presentation of the results from different methods.
776
777 **Fig. 4.** Species tree inferred with *BEAST visualized by using DensiTree (Bouckaert 2010).
778 All trees created in the analysis (except 25 % burn-in phase) are displayed, the consensus
779 trees is highlighted by blue-coloured line. The MCMC analysis ran for 1×10^8 generations, 25
780 % of trees were discarded as a burn-in. The strict molecular clock was chosen for all loci and
781 population function was set as constant. Convergence was assessed by examining the
782 likelihood plots in Tracer v. 1.6 (Rambaut *et al.,* 2014). Bayesian posterior probability (PP)
783 are appended to nodes; only PP ≥ 90 % are shown. The isolates were assigned to a putative
784 species according to the consensual results of the species delimitation methods, i.e, *A. tritici*,
785 *A. candidus*, and two putative species in *A. dobrogensis* lineage (a). Alternativelly, each
786 isolate having unique haplotype was defined as separate species (b).
787
788 **Fig. 5.** Differences between selected phenotypic characters of *Aspergillus candidus* (n=12)
789 and *A. dobrogensis* (n=12). The length and the width of the stipe, and also vesicle diameter
790 were significantly different (Tukey´s HSD test, p value < 0.001) between species, in contrast
791 to diameter of conidia. Boxplots show median, interquartile range, values within ± 1.5 of
792 interquartile range (whiskers) and outliers. Boxplots and violin graphs were created in R 3.3.4
793 (R Core Team 2015) with package *ggplot2* (Wickham 2009).
794
795 **Fig. 6.** Macromorphology and micromorphology of *Aspergillus dobrogensis*. (a–d) Colonies
796 on MEA, CYA, CZA and CY20S (from the right to left) incubated 14 d at 25 °C. (e–h)
797 Biseriate conidiophores. (i) Conidia. (j) Sclerotia. Bar = 10 µm (e–i).

Table 1. List of section *Candidi* strains examined in this study

Species	Strain No.*	Provenance (locality, substrate, year of isolation, collector)	GenBank/EMBL accession Nos.†			
			ITS rDNA	*benA*	*CaM*	*RPB2*
A. campestris	CBS 348.81^T = IMI 259099^T = NRRL 13001^T = IBT 13382^T = ATCC 44563^T = IFM 50931^T = CCF 5596^T	USA, North Dakota, near Zap, storage pile of topsoil displaced from a native, mixed prairie (*Agropyron* spp., *Bouteloua gracilis*), 1979, R.M. Miller & S.M. Pippen	EF669577	EU014091	EF669535	EF669619
A. candidus	CBS 566.65^T = IMI 091889^T = NRRL 303^T = IBT 14006^T = IBT 28566^T = ATCC 1002^T = CCF 5594^T	unknown, received by Raper and Fennell in 1909 from Prof. Westerdijk	EF669592	EU014089	EF669550	EF669634
	CCF 488 = IBT 32273	Czech Republic, tunnels of bark beetles, 1960, E. Sychrová	**FR733811**	**LT626977**	**LT626978**	**LT626979**
	CCF 4029 = CMF ISB 1730 = IBT 32272	Romania, Meziad Cave, bat droppings, 2009, A. Nováková	**FR733813**	**LT626980**	**FR751424**	**LT626981**
	CCF 3996 = CBS 134394 = IBT 33369	Czech Republic, Prague, external auditory canal of 53-year-old man (otitis externa), 2010, P. Lysková	FR727137	FR775325	HE716843	**LT626982**
	CCF 5577 = IBT 33370	Romania, Ungurului Cave, old bat guano, 2010, A. Nováková	**LT626946**	**LT626983**	**LT626984**	**LT626985**
	NRRL 58579 = CCF 5843 = IBT 33371 = EMSL No. 914	USA, New York, indoor air of a home, 2008, Ž. Jurjević	**LT626947**	**LT626986**	**LT626987**	**LT626988**
	NRRL 58959 = CCF 5845 = EMSL No. 1252	USA, Pennsylvania, indoor air of a home, 2009, Ž. Jurjević	**LT626948**	**LT626989**	**LT626990**	**LT626991**
	CCF 4912 = IBT 33373 = EMSL No. 2295	USA, New Jersey, Cranbury, crawlspace metal duct (swab), 2014, Ž. Jurjević	**LT626949**	**LT626992**	**LT626993**	**LT626994**
	CCF 4713 = IBT 33367	Romania, Ungurului Cave, bat guano, 2010, A. Nováková	**LT626950**	**LT626995**	**LT626996**	**LT626997**
	CCF 4659	Czech Republic, Hustopeče, toenail of 52-year-old woman, 2012, S. Dobiášová	HG915889	HG916672	HG916681	**LT626998**
	CCF 4915 = EMSL No. 1285	USA, Rhode Island, indoor air of living room, 2009, Ž. Jurjević	**LT626951**	**LT626999**	**LT627000**	**LT627001**
	NRRL 4646 = IMI 359076 = DTO 213-G2 = CBS 133061	USA, barn litter, D. Fennell	EF669605	EU014090	EF669563	EF669647
	CCF 5675 = IBT 33604 = EMSL No. 2403	USA, Pennsylvania, Feasterville, indoor air (basement of a house), 2014, Ž. Jurjević	**LT626952**	**LT627002**	**LT627003**	**LT627004**
	CCF 5172	Czech Republic, Prague, mouse excrements in seed store, 2000, J. Hubert	**LT626953**	**LT627005**	**LT627006**	**LT627007**
	CCF 5576 = EMSL No. 2421	USA, New York, Binghamton, air in bedroom, 2014, Ž. Jurjević	**LT626954**	**LT627008**	**LT627009**	**LT627010**
	DTO 223-E5	The Netherlands, soil, 2012, M. Meijer	**LT626955**	**LT627011**	**LT627012**	**LT627013**
A. dobrogensis	CCF 4651^T = CCF 4655^T = NRRL 62821^T = IBT 32697^T = CBS 143370^T	Romania, Movile Cave, 2nd airbell, cave sediment, 2012, A. Nováková	**LT626959**	**LT627027**	**LT558722**	**LT627028**
	CCF 5567	Romania, Meziad Cave, bat droppings, 2009, A. Nováková	**LT626960**	**LT627029**	**LT627030**	**LT627031**
	CCF 5568	Romania, Liliecilor de la Guru Dobrogei Cave, Galeria Fossile, bat guano, 2010, A. Nováková	**LT626961**	**LT627032**	**LT627033**	**LT627034**
	CCF 4650 = CCF 4657 = NRRL 62820 = IBT 32699	Romania, Meziad Cave, cave sediment, 2010, A. Nováková	**LT626962**	**LT627035**	**LT627036**	**LT627037**
	CCF 4649 = IBT 32700	Romania, Liliecilor de la Gura Dobrogei Cave, Galeria Fossile, bat guano, 2010, A. Nováková	**LT626963**	**LT627038**	**LT627039**	**LT627040**

	CCF 5569	Romania, Liliecilor de la Gura Dobrogei Cave, Galeria Fossile, bat guano, 2010, A. Nováková	**LT626964**	**LT627041**	**LT627042**	**LT627043**
	CCF 5570	Romania, Liliecilor de la Gura Dobrogei Cave, Galeria Fossile, bat droppings, 2010, A. Nováková	**LT626965**	**LT627044**	**LT627045**	**LT627046**
	CCF 5573	Romania, Liliecilor de la Gura Dobrogei Cave, cave air, 2011, A. Nováková	**LT626966**	**LT627047**	**LT627048**	**LT627049**
	CCF 5571	Romania, Meziad Cave, hall in the upper floor, bat guano, 2010, A. Nováková	**LT626967**	**LT627050**	**LT627051**	**LT627052**
	CCF 5572	Romania, Liliecilor de la Gura Dobrogei Cave, cave air, 2013, A. Nováková	**LT626968**	**LT627053**	**LT627054**	**LT627055**
	CCF 5574	Romania, Liliecilor de la Gura Dobrogei cave, Galeria Fossile, bat droppings, 2014, A. Nováková	**LT626969**	**LT627056**	**LT627057**	**LT627058**
	CCF 5575	Czech Republic, nails of 31-year-old woman, 2014, P. Lysková	**LT626970**	**LT627059**	**LT627060**	**LT627061**
	CBS 225.80 = DTO 031-E6	The Netherlands, human nail (contaminant), 1980	**LT626971**	**LT627062**	**LT627063**	**LT627064**
	DTO 025-I1	Germany, carpet, 2006	**LT626972**	**LT627077**	**LT627078**	**LT627079**
	DTO 013-C4 = IBT 28582	The Netherlands, Maastricht, indoor air, 2006, J. Houbraken	**LT626973**	**LT627065**	**LT627066**	**LT627067**
	DTO 001-F9 = IBT 28576	The Netherlands, surface of object in museum, 2004, J. Houbraken	**LT626974**	**LT627068**	**LT627069**	**LT627070**
	DTO 029-H2	Germany, carpet, 2006	**LT626975**	**LT627071**	**LT627072**	**LT627073**
	DTO 031-D9 = CBS 116945 = IBT 116945 = IBT 28573	The Netherlands, Tiel, dust in museum, 2004, J. Houbraken	**LT626976**	**LT627074**	**LT627075**	**LT627076**
	CCF 5844 = EMSL No. 2810	USA, New York, Lockport, indoor air in basement (settle plate), 2015, Ž. Jurjević	**LT907963**		**LT907965**	**LT907968**
	IBT 29476 = CCF 5823	Denmark, Høve Strand, mouse dung (in bed in summer house annex), 2007, J.C. Frisvad	**LT907964**	**LT907967**	**LT907966**	**LT907969**
	FMR 15444 = CBS 142752	Spain, Galicia, Lugo, Ribeira Sacra, herbivore dung, 2016, J. Guarro & M. Guevara-Suarez	**LT798904**	**LT798921**	**LT798922**	**LT798923**
	FMR 15601 = CCF 5846	Spain, Galicia, Orense, Cortegada, herbivore dung, 2016, J. Guarro & M. Guevara-Suarez		**LT962396**		
A. pragensis	CCF 3962^{T} = CBS 135591^{T} = IBT 32274^{T} = NRRL 62491^{T}	Czech Republic, Prague, toenail of 58-year-old man, 2007, M. Skořepová	FR727138	HE661604	FR751452	LN849445
	CCF 4654 = NRRL 62822 = IBT 32701	Czech Republic, Prague, toenail of 59-year-old man, 2013, P. Lysková	HG915888	HG916673	HG916680	**LT627014**
	CCF 4911 = NRRL 58614 = EMSL No. 1057	USA, Pennsylvania, indoor air of a home, 2008, Ž. Jurjević	**LT908111**	**LT908037**	**LT908038**	**LT908039**
	CCF 5847 = EMSL No. 2216	USA, Pennsylvania, Feasterville, carpet in bedroom, 2013, Ž. Jurjević	**LT908112**	**LT908040**	**LT908041**	**LT908042**
	CCF 5693 = EMSL No. 2397	USA, Maryland, Cohasset, outdoor air, 2014, Ž. Jurjević	**LT908113**	**LT908043**	**LT908044**	**LT908045**
A. subalbidus	CBS 567.65^{T} = NRRL 312^{T} = ATCC 16871^{T} = IMI 230752^{T} = CCF 5822	Brazil, received by Raper and Fennell in 1939 from J. Reis (Instituto Biologica)	EF669593	KP987050	EF669551	EF669635
	CBS 112449 = DTO 031-E3 = DTO 039-E7	Germany, indoor environment	**LT626956**	EU076294	EU076307	**LT627015**
	NRRL 5214 = ATCC 26930 = IMI 16046 = CCF 4860	Ghana, vegetable lard, International Mycological Institute, Egham, England, 1933, sent by H.A. Dade to IMI collection	**LT908114**	**LT908034**	**LT908035**	**LT908036**
A. taichungensis	IBT 19404^{T} = PF 1167^{T} = CCF 5597^{T}	Taiwan, Taichung city, soil, 1994, T. Yaguchi	**LT626957**	EU076297	HG916679	**LT627016**

A. tritici	CBS 266.81^{T} = IBT 21956^{T} = CCF 5842^{T}	India, grains of *Triticum aestivum*, < 1976, B.S. Mehrotra	**LT626958**	EU076293	HG916678	**LT627017**
	CCF 4030 = CMF ISB 1300 = IBT 32729	Czech Republic, Frýdek-Místek, vermicompost, 2001, A. Nováková	**FR733814**	**LT627018**	**FR751425**	**LT627019**
	CCF 4653	Czech Republic, Prague, toenail of 58 -year-old woman, 2012, P. Lysková	HG915890	HG916674	HG916677	**LT627020**
	CCF 3853 = IBT 32725	Czech Republic, Prague, toenail of 62-year-old man, 2008, M. Skořepová	FR727136	FR775327	HE661598	**LT627021**
	CCF 3314	Czech Republic, Prague, outdoor air, 1996, A. Kubátová	**FR733812**	**LT627022**	**FR751426**	**LT627023**
	CCF 1649	Czech Republic, Prague, flour, 1979, J. Svrčková	**FR733810**	**LT627024**	**FR751427**	**LT627025**
	CCF 4658	Czech Republic, Prague, toenail of 69-year-old woman, 2008, M. Skořepová	HG915891	HG916675	HG916676	**LT627026**

[*] Acronyms of culture collections in alphabetic order: ATCC, American Type Culture Collection, Manassas, Virginia; CBS, CBS culture collection housed at the Westerdijk Institute, Utrecht, The Netherlands; CCF, Culture Collection of Fungi, Department of Botany, Charles University, Prague, Czech Republic; CMF ISB, Collection of Microscopic Fungi of the Institute of Soil Biology, Academy of Sciences of the Czech Republic, České Budějovice, Czech Republic; DTO, working collection of the Applied and Industrial Mycology department housed at the Westerdijk Institute, Utrecht, The Netherlands; EMSL, EMSL Analytical Inc., New Jersey, USA; FRR, Food Fungal Culture Collection, North Ride, Australia; IFM, Collection at the Medical Mycology Research Center, Chiba University, Japan; IFO, Institute for Fermentation, Osaka, Japan; IHEM, Belgian Coordinated Collections of Micro-organisms (BCCM/IHEM), Brussels, Belgium; IMI, CABI's collection of fungi and bacteria, Egham, UK; NRRL, Agricultural Research Service Culture Collection, Peoria, Illinois, USA

[†] Sequences deposited in this study are in bold print

Table 2. Comparison of selected morphological characters between *Aspergillus candidus* and *A. dobrogensis*

Morphological character	***A. candidus***		***A. dobrogensis***	
	Range	**Average ± standard deviation**	**Range**	**Average ± standard deviation**
Length of conidiophore* (µm)	(85–)120–1200(–1800)	368 ± 318	(125–)150–2200(–3000)	880 ± 610
Width of stipe* (µm)	(3–)3.5–11(–14)	6.4 ± 2.1	(3.5–)4–13(–15)	8.1 ± 2.6
Diameter of vesicle* (µm)	(7–)8–29(–42)	16 ± 6.2	(8–)9–31(–36)	18.6 ± 6.4
Diameter of conidia (µm)	3.5–5	4.1 ± 0.3	(3–)3.5–5(–5.5)	4 ± 0.3
Colony diam: MEA, 14 d, 25 °C (mm)	19–34	26 ± 4	21–37	30 ± 3
Colony diam: MEA, 14 d, 30 °C (mm)	17–28	22 ± 4	22–25	23 ± 1
Colony diam: MEA, 14 d, 33 °C (mm)	0–15	8 ± 5	2–9	4 ± 2
Colony diam: MEA, 14 d, 35 °C (mm)	0–4	2 ± 1	0	0
Colony diam: MEA, 14 d, 37 °C (mm)	0	0	0	0
Colony diam: CYA, 14 d, 25 °C (mm)	25–37	31 ± 3	30–46	39 ± 3
Colony diam: CZA, 14 d, 25 °C (mm)	19–27	24 ± 2	21–33	27 ± 3
Colony diam: CY20S, 14 d, 25 °C (mm)	24–45	32 ± 5	32–48	40 ± 5

* Excluding diminutive conidiophores

Table 3. Exometabolites found in *Aspergillus candidus* and *A. dobrogensis*

	Species, isolate numbers														
	A. candidus								***A. dobrogensis***						
Exometabolite[*, †]	CBS 566.65[T]	CCF 488	CCF 3996	NRRL 58579	CCF 4912	CCF 5577	CCF 4713	CCF 5675	CCF 4651[T]	IBT 29476	CCF 4649	CCF 4650	DTO 013-C4	DTO 001-F9	CBS 116945
Aspergilazine A	+			+	+			+							
Barceloneic acid C	+					+		+							
Brevianamide F	+	+	+	+	+	+	+	+	+	+	+		+	+	+
Candidusin A	+														
Candidusin B	+	+													
Chlorflavonin	+	+	+	+	+	+	+	+	+	+	+	+	+	+	+
Sphaeropsidin A		+						+				+	+		
Terphenyllin	+	+	+												
3-Hydroxyterphenyllin	+	+	+												
12,13-DDB E[‡]		+	+			+	+		+	+			+	+	+
12,13-DDB E[‡] derivative 1									+	+			+	+	+
12,13-DDB E[‡] derivative 2									+	+			+	+	+
12,13-DDB E[‡] derivative 3									+	+			+	+	+
12,13-DDB E[‡] derivative 4									+	+					
“ALKO”				+	+		+	+							
“AQ RED 1”[§]										+			+	+	+
“AQ RED 2”[§]														+	+
“Aspergiloid1”													+	+	+
“Aspergiloid2”													+	+	+
“Aspergiloid3”											+	+	+		+
“Aspergiloid3a”														+	+
“Aspergiloid4”									+	+			+		
“Aspergiloid5”			+	+	+	+	+			+			+	+	
“FMI”													+	+	+
“MOYN”				+	+		+								
“MYO”	+			+	+		+								
“Paspa1”	+								+	+			+	+	+
“Paspa2”	+			+		+		+	+	+			+	+	+
“Paspa3”													+	+	+
“Paspa4”														+	+
“TAROT”												+	+		
“TAROT2”													+		
“TUT”		+			+	+		+							
“VERN2”													+		
“Indole alkaloid 1”												+		+	
“An extrolite with a benzomalvin chromophore”													+		

[*] The metabolite names in quotes are characterized by a characteristic UV spectrum, but their structure has not been elucidated

[†] Absorption maxima and alkylphenone retention indexes of all detected exometabolites are listed in Table S1

[‡] 12,13-dehydrodesoxybrevianamide E

[§] A red anthraquinone-like extrolite

Table 4. Antifungal susceptibility profiles of *Aspergillus* section *Candidi* members determined by EUCAST 9.3 reference method.

Species (No. of tested isolates)	MICs (mg L^{-1})*											
	Terbinafine		Posaconazole		Isavuconazole		Voriconazole		Itraconazole		Amphotericin B	
	Range	GM*	Range	GM	Range	GM	Range	GM	Range	GM	Range	GM
A. campestris (1)	0.125	–	≤0.03	–	2	–	1	–	≤0.125	–	1	–
A. candidus (14)	≤0.03–4	0.26	≤0.03–0.5	0.09	≤0.125–2	0.48	≤0.125–1	0.61	≤0.125–0.5	0.26	0.06–1	0.21
A. dobrogensis (13)	≤0.03–0.25	0.12	≤0.03–0.5	0.16	0.125–2	0.45	0.5–1	0.81	≤0.125–0.5	0.21	0.125–1	0.20
A. pragensis (5)	0.06–0.25	–	≤0.03–0.5	–	≤0.125–2	–	≤0.125–1	–	≤0.125–0.25	–	0.06–0.5	–
A. subalbidus (3)	0.06–4	–	0.06	–	2	–	1–2	–	0.25–0.5	–	0.25–1	–
A. taichungensis (1)	0.5	–	≤0.03	–	2	–	2	–	≤0.125	–	1	–
A. tritici (7)	0.125–0.5	–	≤0.016–0.125	–	≤0.03–2	–	≤0.06–1	–	≤0.016–0.25	–	0.06–1	–
All isolates (44)	≤0.03–4	0.19	≤0.03–0.125	0.09	≤0.125–2	0.45	≤0.125–2	0.56	≤0.125–0.5	0.19	0.06–1	0.22

*In order to calculate the GM (geometric mean) and MIC (minimum inhibitory concentration), off-scale MICs (≤ 0.03 and ≤ 0.125 mg/L) were translated to 0.03 and 0.125, although recognising that this may lead to a slight overestimation of the actual values. GM was calculated for >10 isolates tested per species.

Figure 1 colour online

Click here to download Figure Fig. 1 colour online.eps

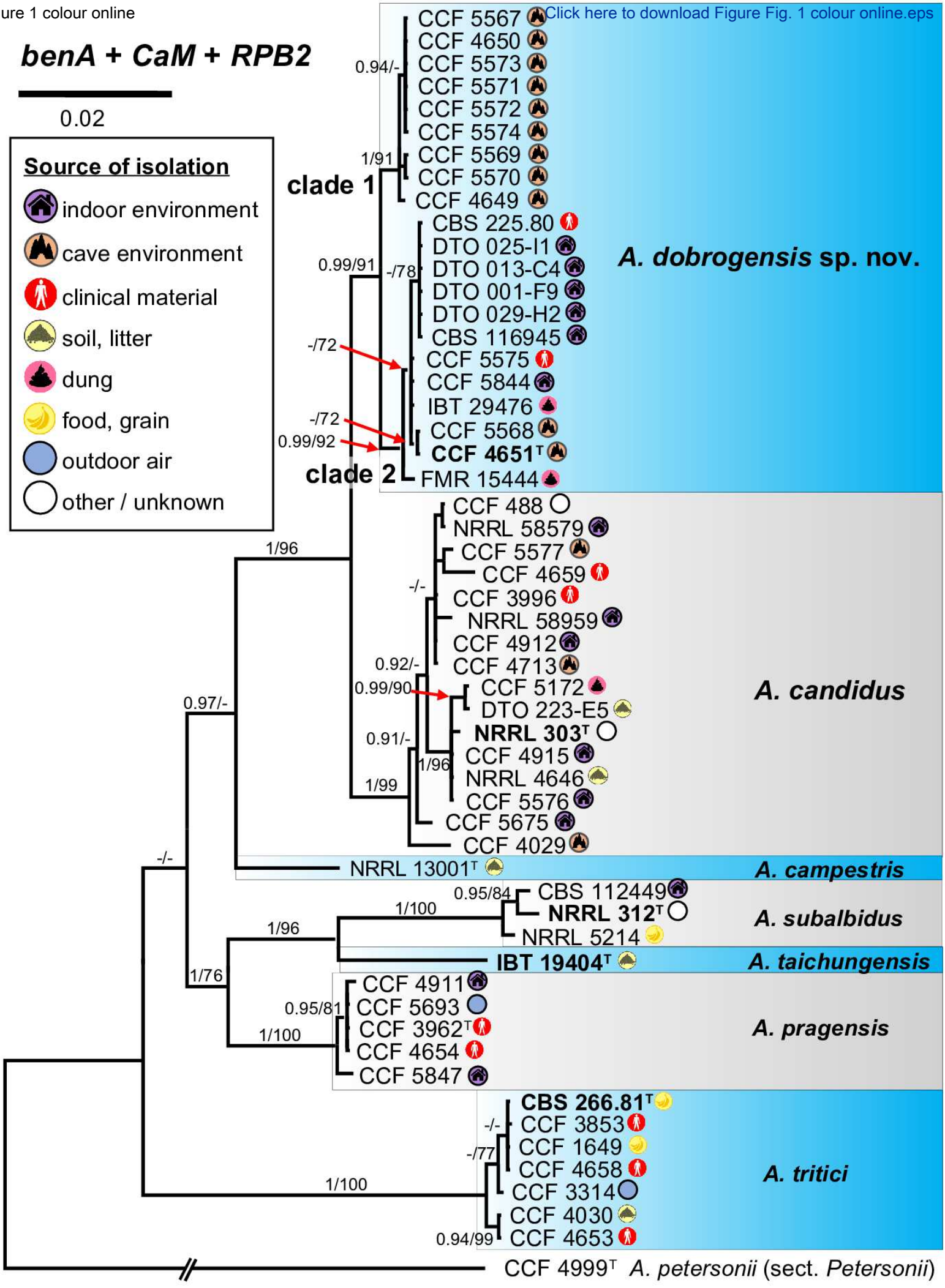

Figure 1 grayscale print

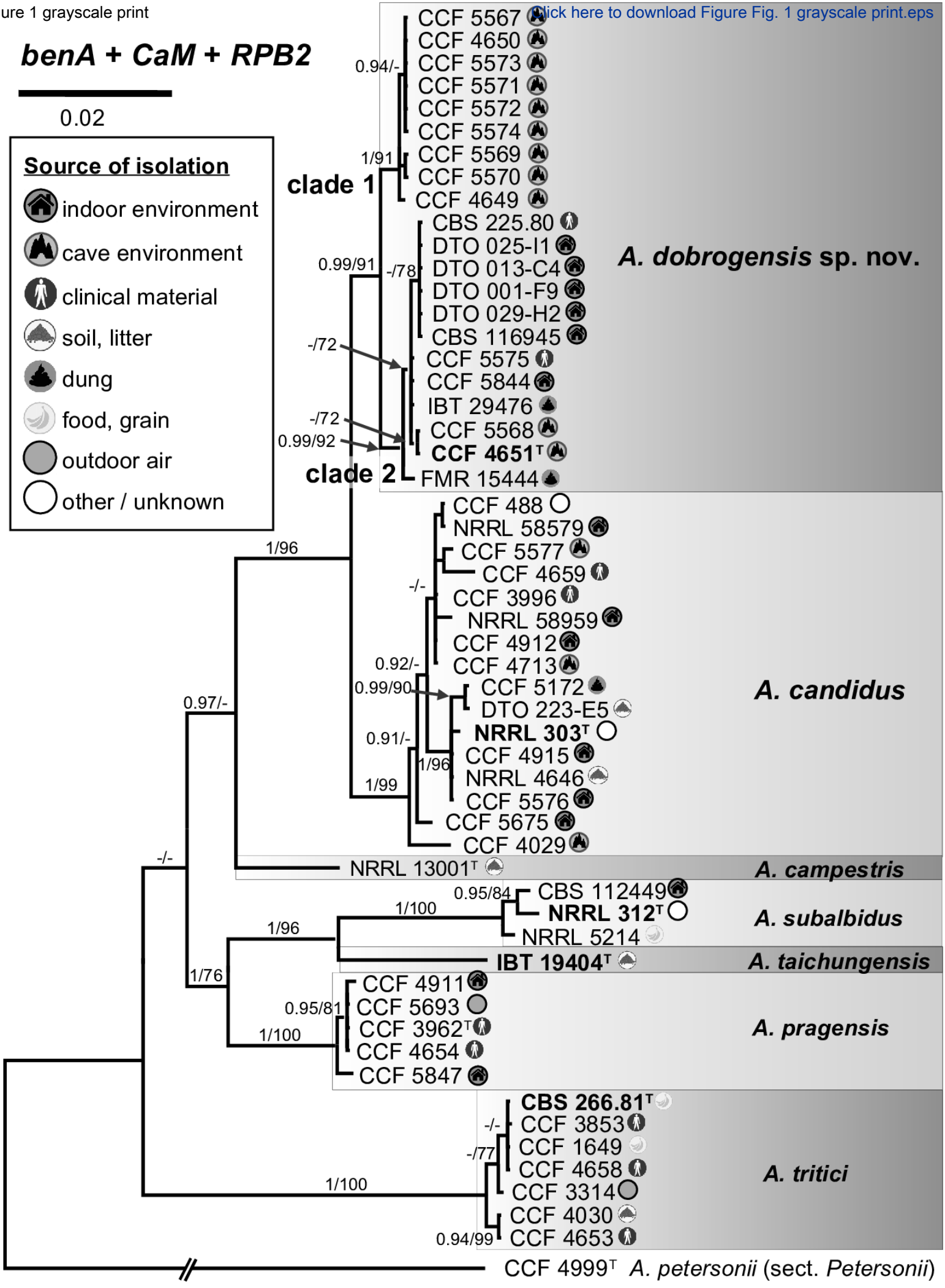

Figure 2 colour online

Click here to download Figure Fig. 2 colour online.tif

Figure 2 grayscale print

Click here to download Figure Fig. 2 grayscale print.tif

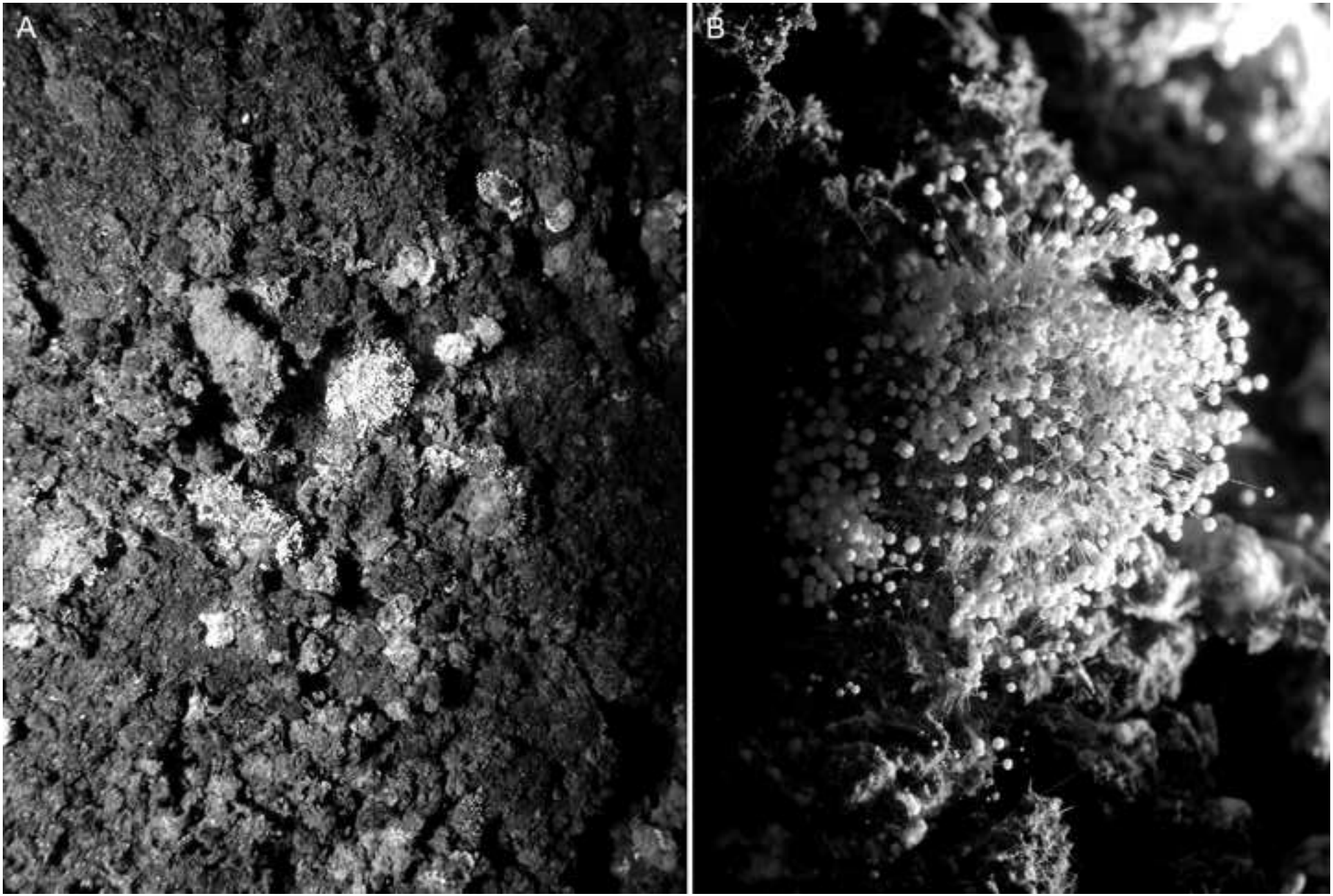

Figure 3 colour online

Click here to download Figure Fig. 3 colour online.eps

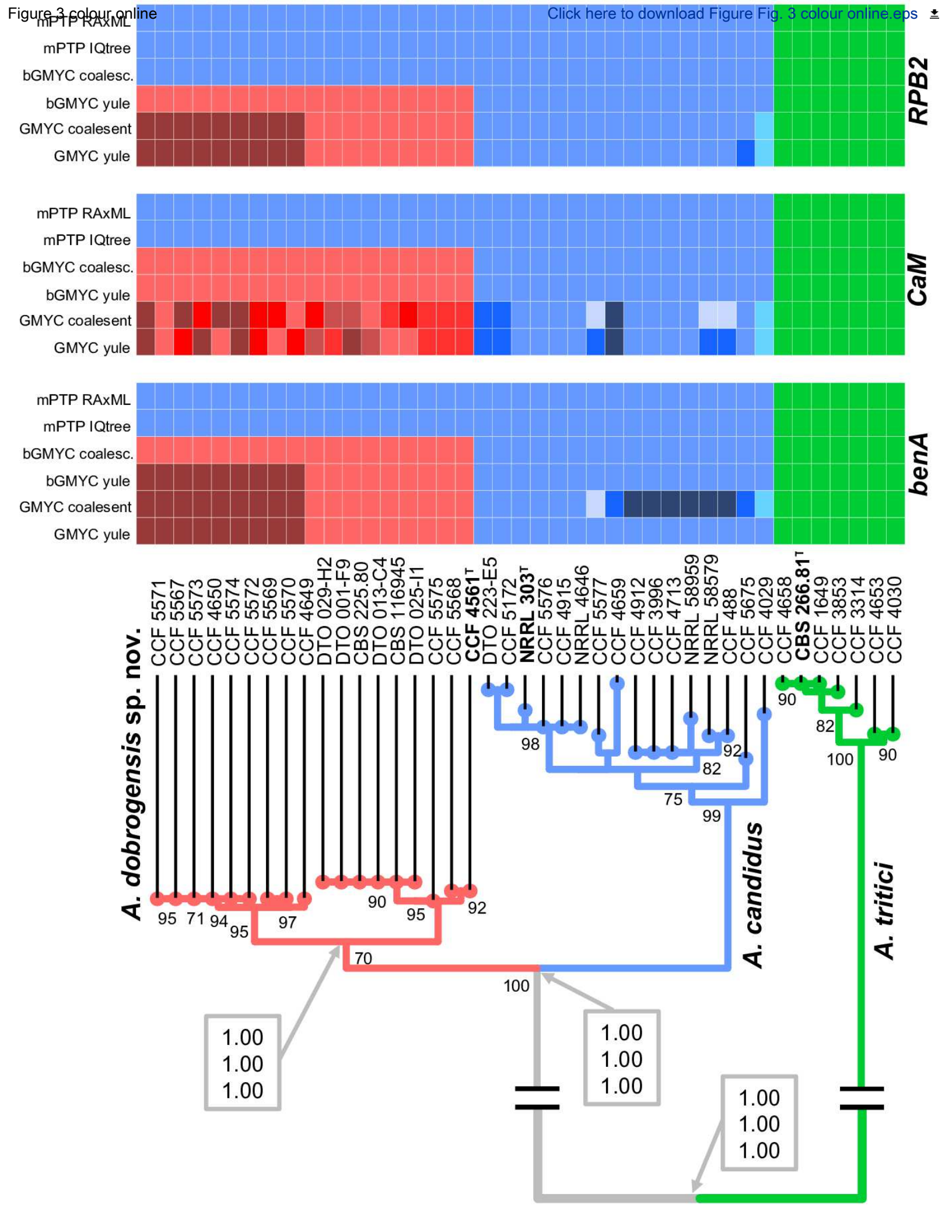

Figure 3 grayscale print

Click here to download Figure Fig. 3 grayscale print.eps

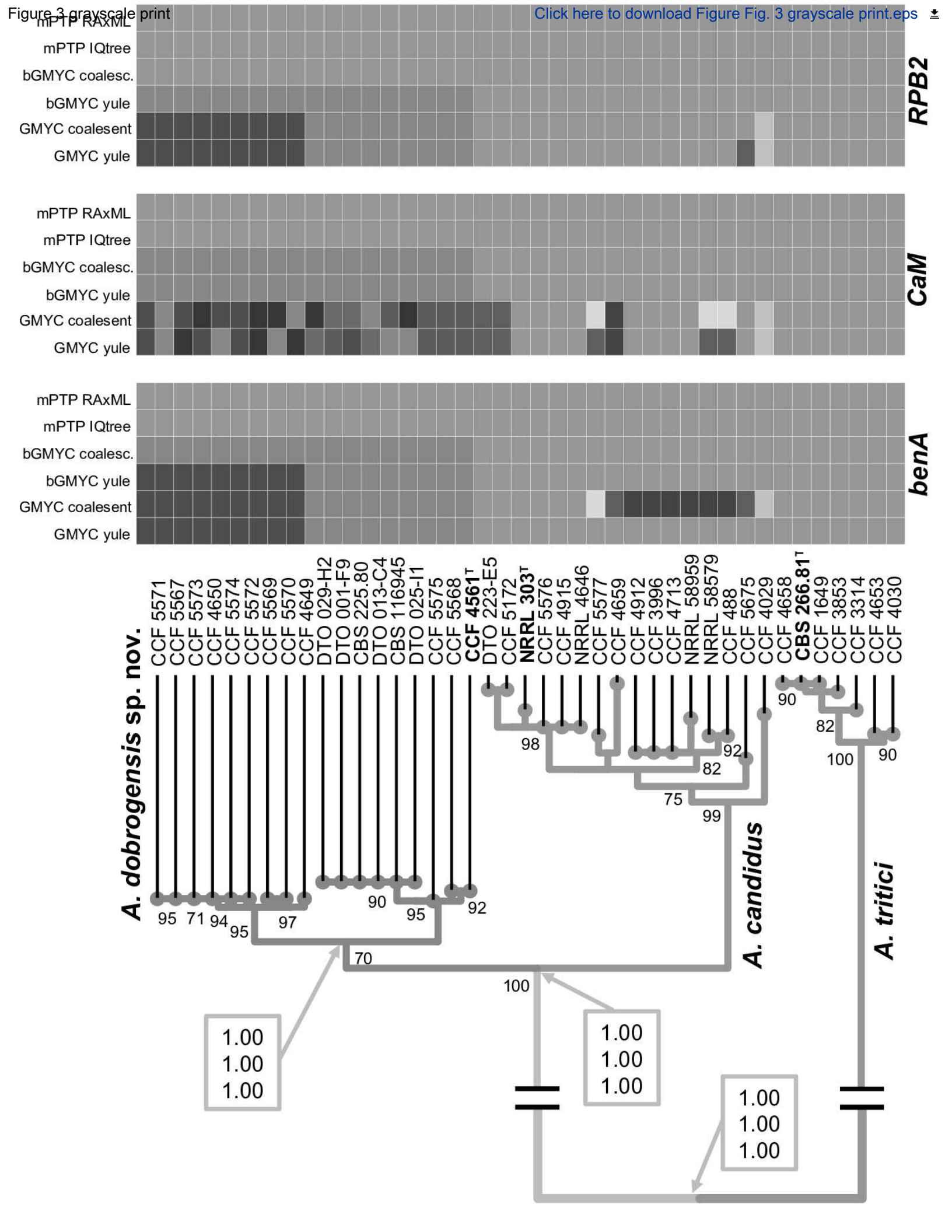

Figure 4 colour online

Click here to download Figure Fig. 4 colour online.eps

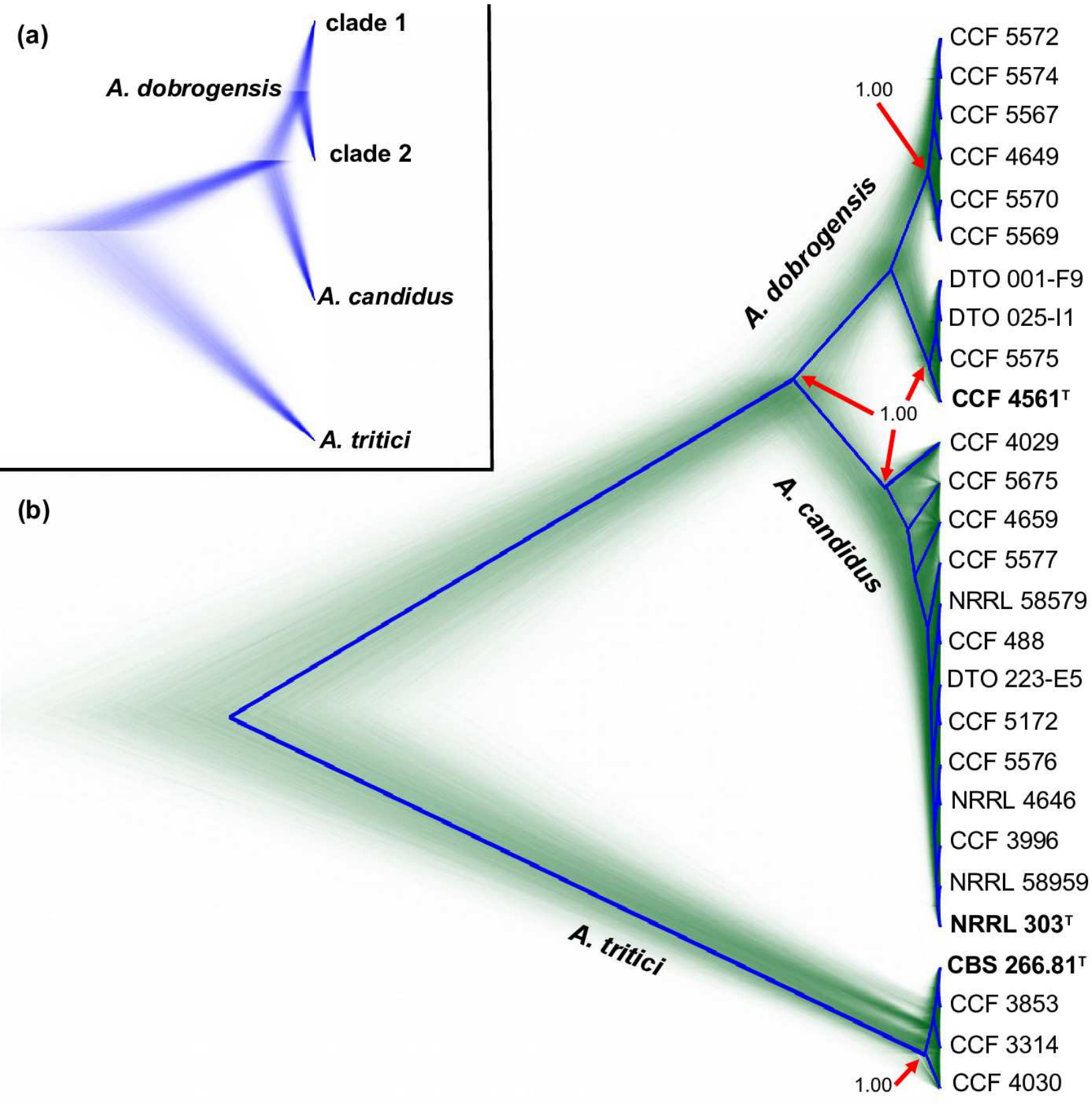

Figure 4 grayscale print

Click here to download Figure Fig. 4 grayscale print.eps

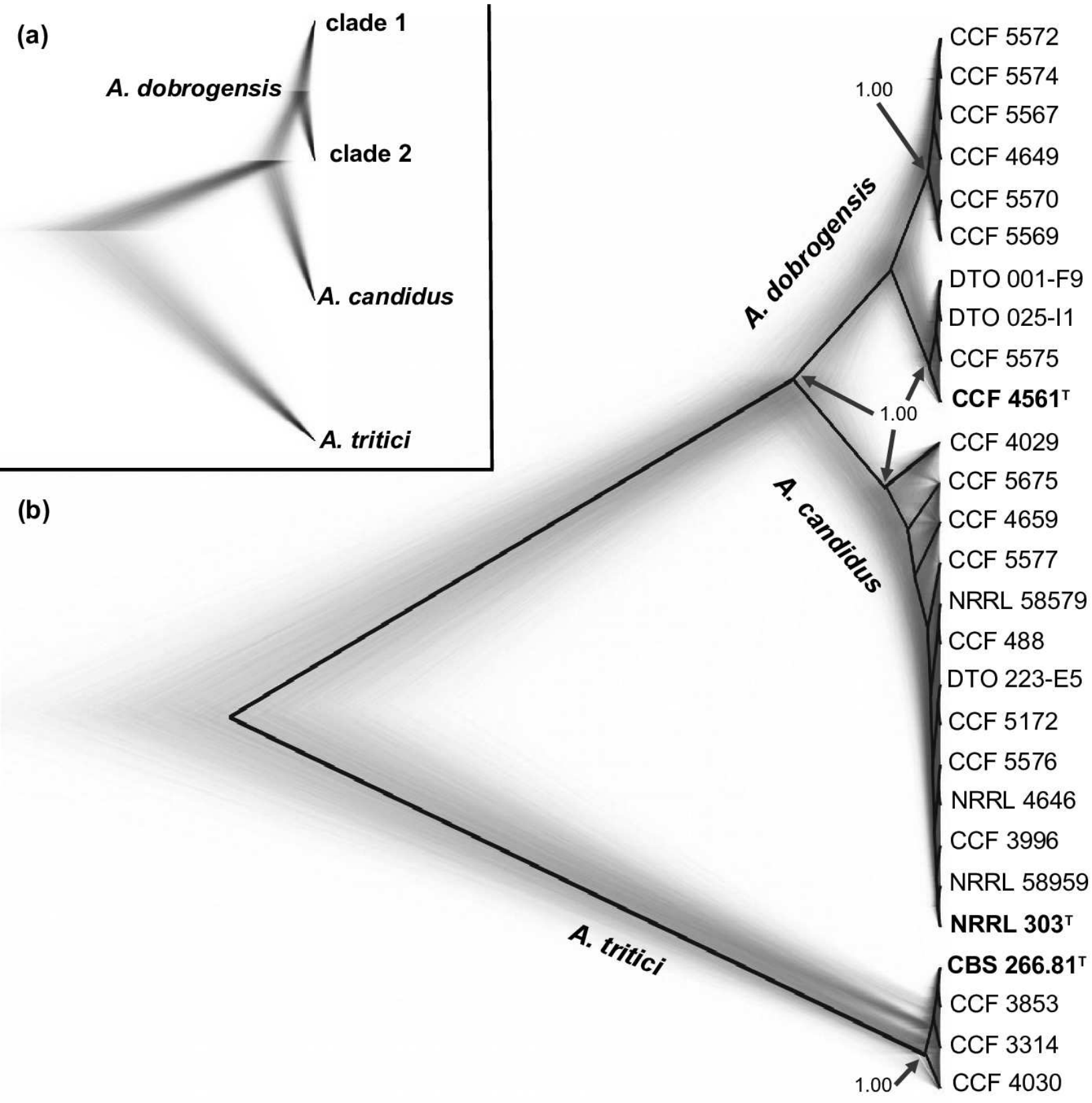

Figure 5 colour online

Click here to download Figure Fig. 5 colour online.eps

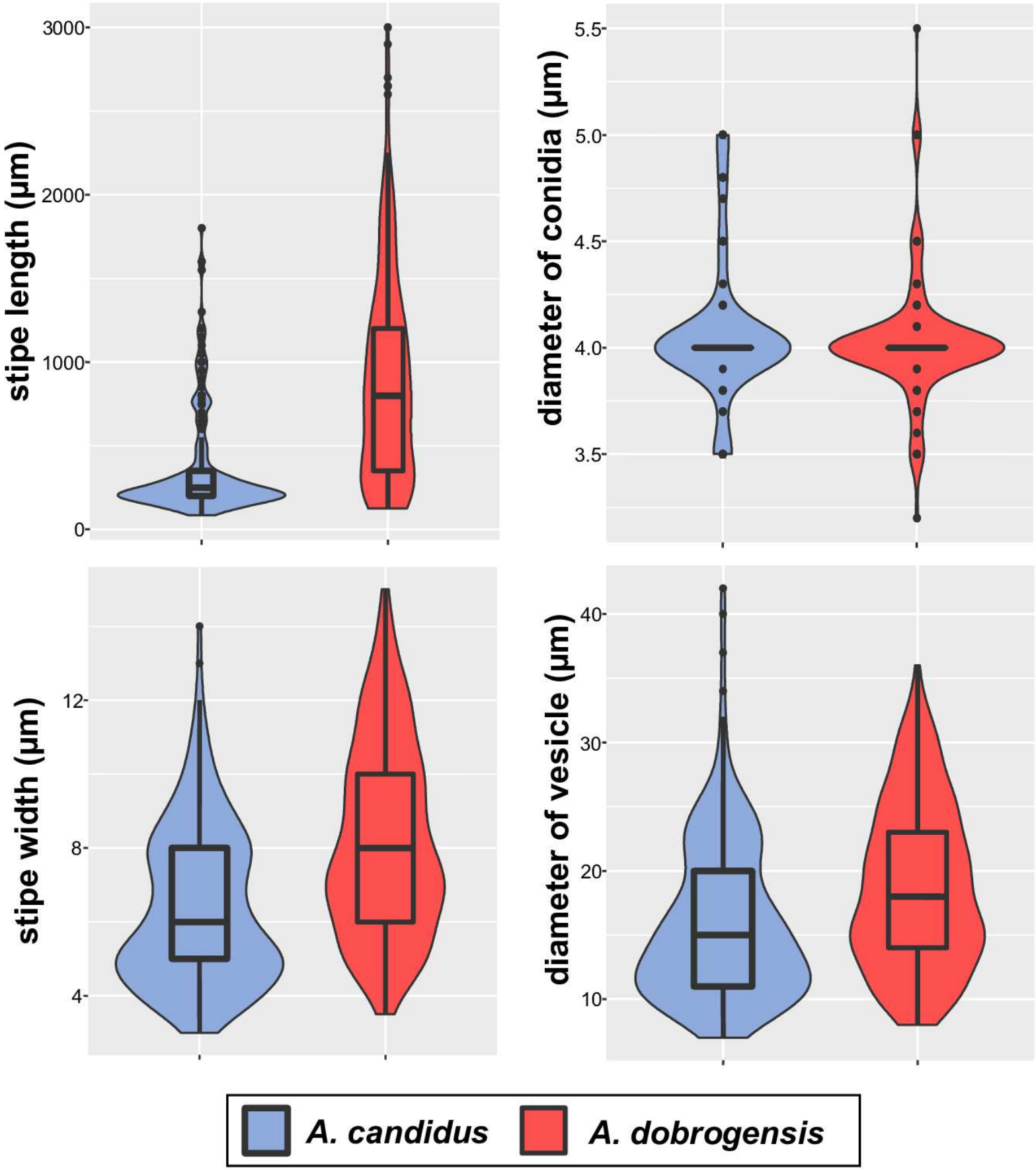

Figure 5 grayscale print

Click here to download Figure Fig. 5 grayscale print.eps

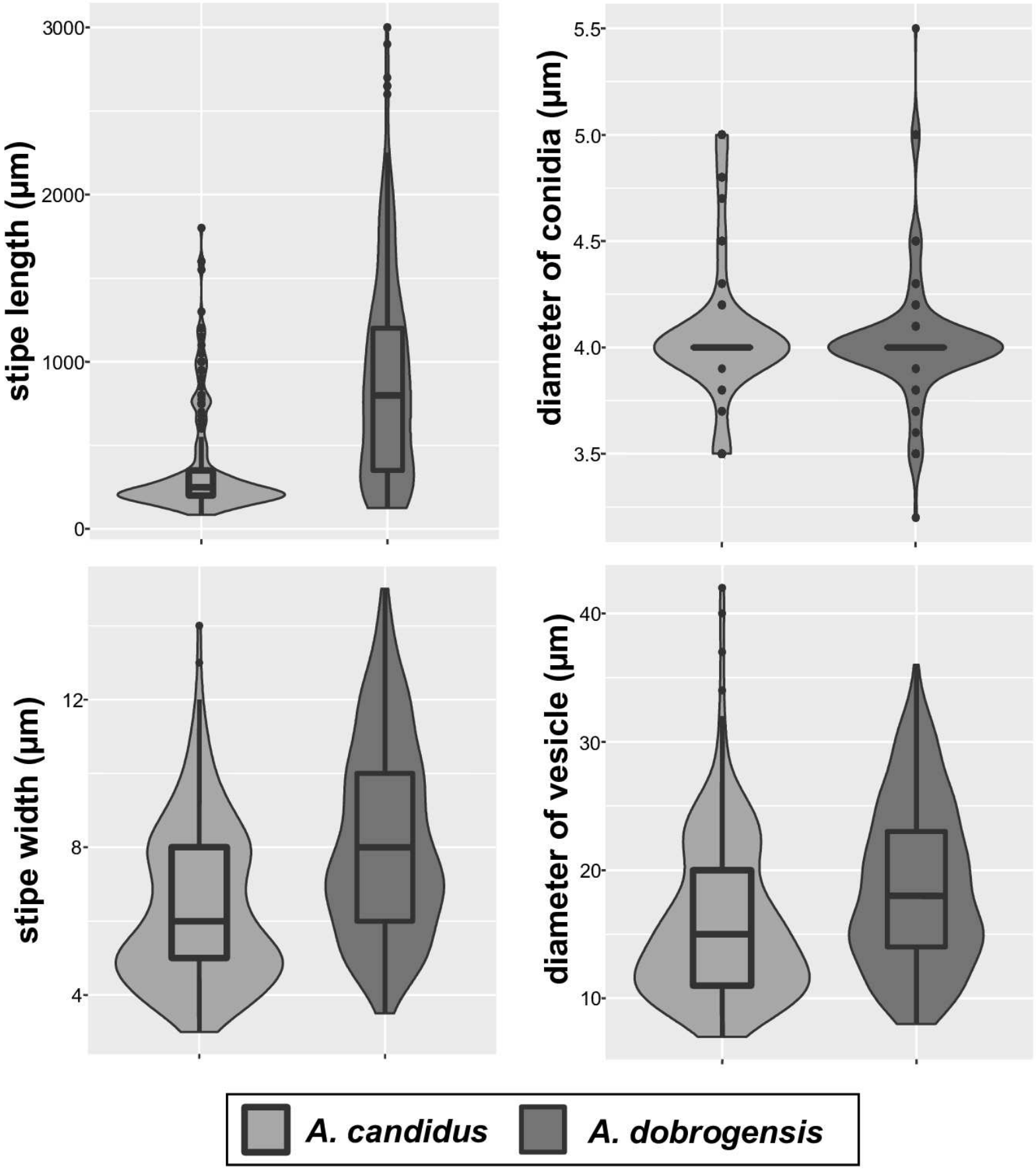

Figure 6 colour online

Click here to download Figure Fig. 6 colour online.tif

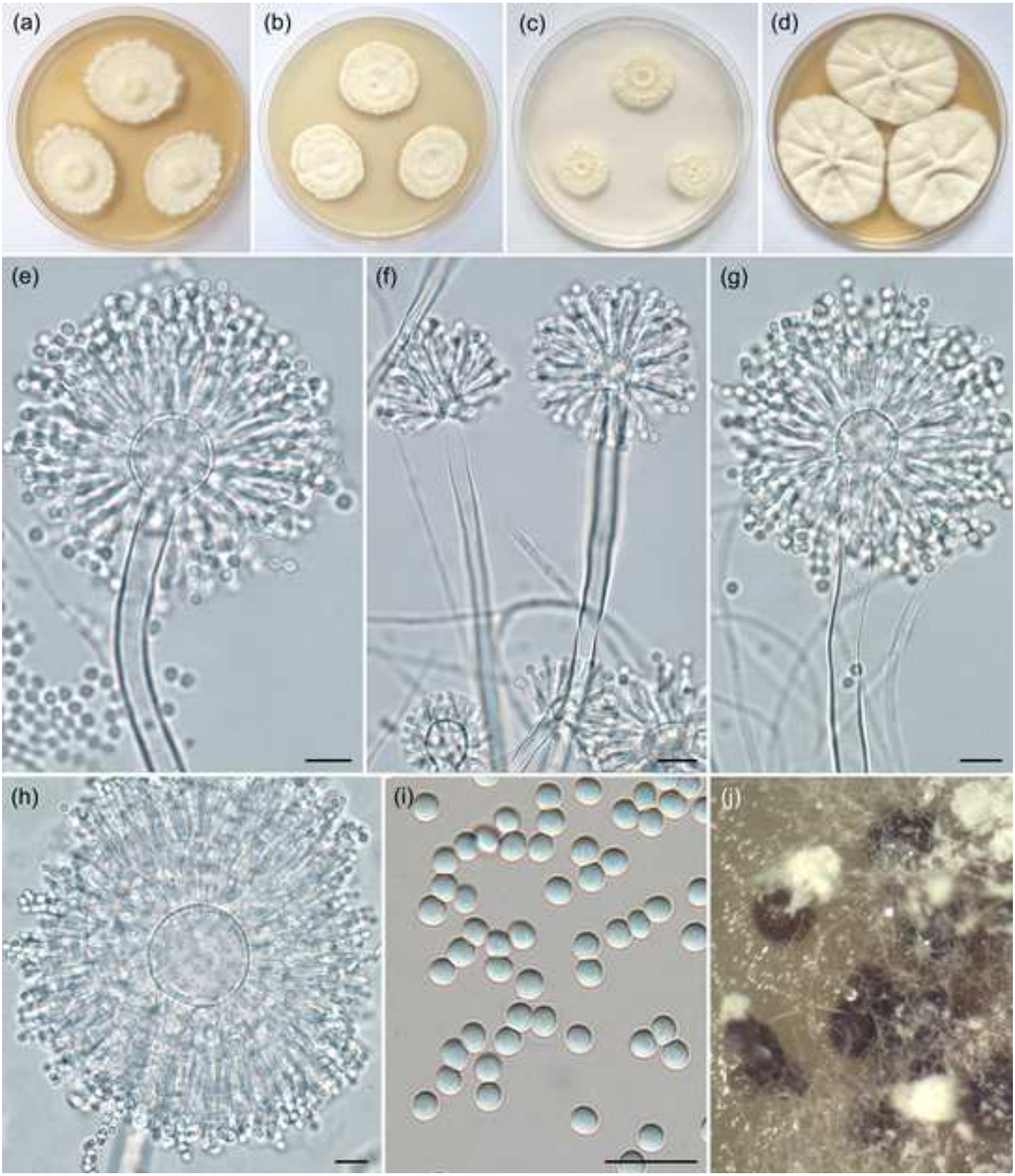

Figure 6 grayscale print

Click here to download Figure Fig. 6 grayscale print.tif

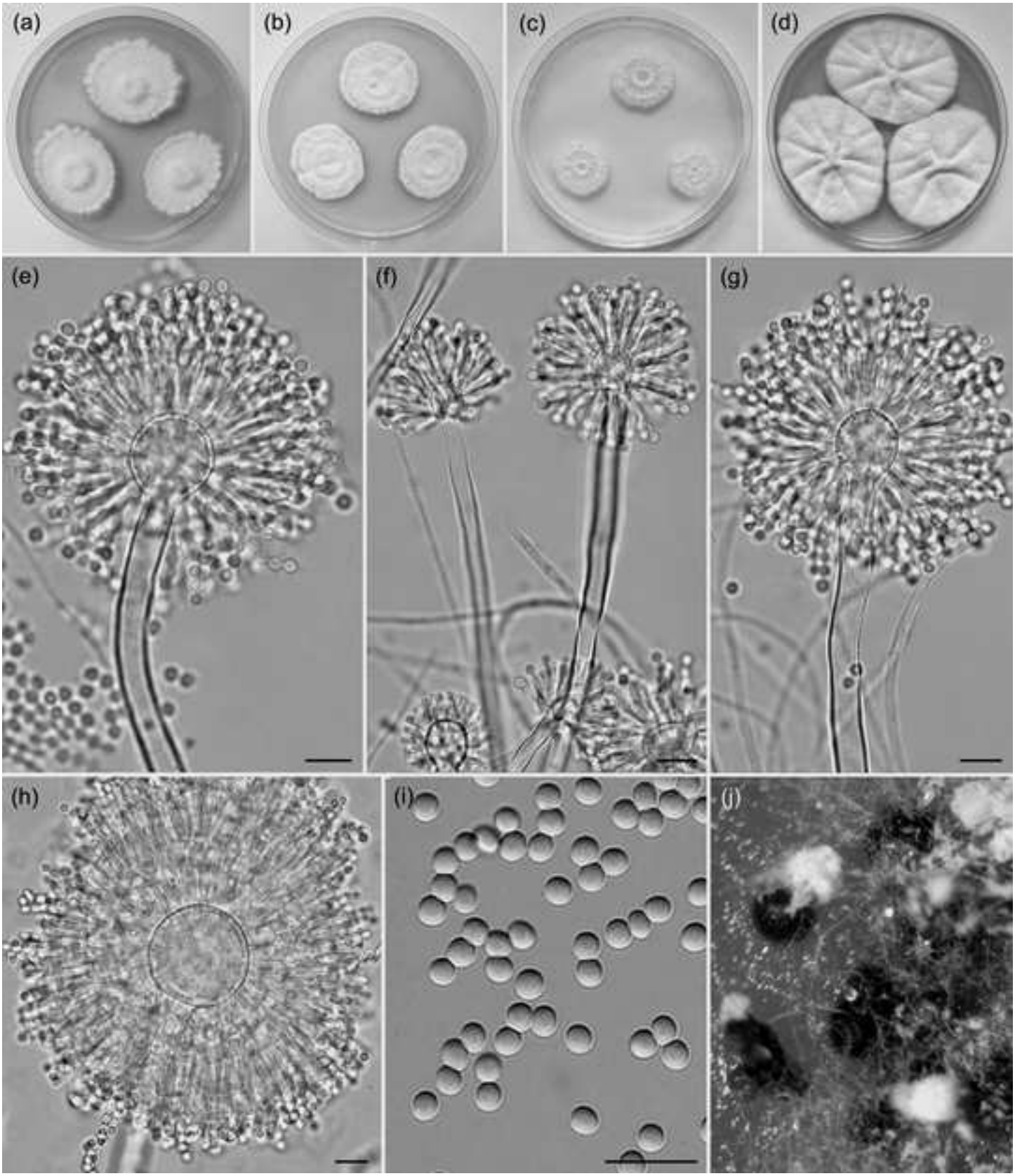

Table S1. Retention indices and UV absorption maxima for extrolites detected in *Aspergillus candidus* and *A. dobrogensis*

Exometabolite[*]	**Alkylphenone retention index**[†]	**UV absorption maxima (nm)**[‡]
Aspergilazine A	767	200, 216, 275sh, 282, 293sh
Barceloneic acid C	781	193, 225, 244, 275
Brevianamide F	720	220, 275sh, 282, 293sh
Candidusins (B, A)	990, 1083	213, 238sh, 280, 295, 334
Chlorflavonin	1053	204, 265, 313sh, 352
Sphaeropsidin A	1078	244
Terphenyllin	869	207, 225sh, 273
3-Hydroxyterphenyllin	819	207, 225sh, 273
12,13-DDB E[§]	697	217, 268
12,13-DDB E[§] derivative 1	766	201, 219, 272
12,13-DDB E[§] derivative 2	777	204, 219sh, 269
12,13-DDB E[§] derivative 3	783	202, 219sh, 265
12,13-DDB E[§] derivative 4	814	193, 218, 281
“ALKO”	924	192, 217, 272
“AQ RED 1”	827	211, 251, 327, 446
“AQ RED 2”	825	223, 278, 365, 432
“Aspergiloid1”	852	298
“Aspergiloid2”	885	204, 245, 320
“Aspergiloid3”	982	204, 220sh, 298
“Aspergiloid3a”	866	200, 300sh, 339
“Aspergiloid4”	994	225, 326
“Aspergiloid5”	1003	230, 253sh, 325
“FMI”	1066	202, 226sh, 299
“MOYN”	787	204, 298
“MYO”	801	202, 242, 297
“Paspa1”	1344	232, 277
“Paspa2”	1355	235, 278
“Paspa3”	1133	218, 270, 310
“Paspa4”	1123	235, 278
“TAROT”	740	215, 250, 302
“TAROT2”	746	215, 250, 302
“TUT”	613	204, 271, 377
“VERN2”	686	208, 291
“Indole alkaloid 1”	677	220, 275sh, 282, 293sh
“An extrolite with a benzomalvin chromophore”	1049	203, 225, 269sh, 276sh, 300sh, 314sh

[*] The metabolites named in quotes have characteristic UV spectra, but none of their structures have been elucidated yet
[†] Determined according to Frisvad & Thrane (1987, 1993)
[‡] sh, shoulder peak
[§] 12,13-dehydrodesoxybrevianamide E

Polyphasic data support the splitting of *Aspergillus candidus* into two species; proposal of *A. dobrogensis* sp. nov.

Running title: Splitting of *Aspergillus candidus*

Vit Hubka[1,2*], Alena Nováková[2], Željko Jurjević[3], František Sklenář[1,2], Jens C. Frisvad[4], Jos Houbraken[5], Maiken C. Arendrup[6], Karin M. Jørgensen[6], João P. Z. Siqueira[7,8], Josepa Gené[8] and Miroslav Kolařík[1,2]

[1] Department of Botany, Faculty of Science, Charles University, Prague, Czech Republic
[2] Laboratory of Fungal Genetics and Metabolism, Institute of Microbiology of the Czech Academy of Sciences, Prague, Czech Republic
[3] EMSL Analytical, Inc., Cinnaminson, New Jersey, USA
[4] Department of Biotechnology and Biomedicine, Technical University of Denmark, Kongens Lyngby, Denmark
[5] Westerdijk Fungal Biodiversity Institute, Utrecht, The Netherlands
[6] Unit of Mycology, Department of Microbiology & Infection Control, Statens Serum Institut, Artillerivej 5, DK-2300, Copenhagen, Denmark
[7]Laboratório de Microbiologia, Faculdade de Medicina de São José do Rio Preto, 5416 Brigadeiro Faria Lima Ave., 15090-000, São José do Rio Preto, Brazil
[8]Unitat de Micologia, Facultat de Medicina i Ciències de la Salut, IISPV, Universitat Rovira i Virgili, Reus, Spain

*****corresponding authors e-mail: hubka@biomed.cas.cz; phone: +420 739663218

Key words: antifungal susceptibility testing, antioxidant compounds, bioprospecting, cave mycobiota, indoor fungi, multispecies coalescence model

contents category: new taxa (Eukaryotic micro-organisms)

The GenBank/ENA/DDBJ accession numbers for the ITS rDNA, β-tubulin, calmodulin and DNA-dependent RNA polymerase II, second largest subunit sequences of the ex-type strain CCF 4651^T of *Aspergillus dobrogensis* are LT626959, LT627027, LT558722 and LT627028, respectively.

The MycoBank (http://www.mycobank.org) accession number for *Aspergillus dobrogensis* is MB821313.

Abbreviations: *benA*, fragment of the β-tubulin gene; BI, Bayesian Inference; *CaM*, fragment of the calmodulin gene; EUCAST, European Committee on Antimicrobial Susceptibility testing; GM, geometric mean; ITS, fragment containing ITS1, 5.8S rDNA and ITS2 region of rDNA; MIC, minimum inhibitory concentration; ML, Maximum Likelihood; MSC, multispecies coalescent model; *RPB2*, fragment of the DNA-dependent RNA polymerase II, second largest subunit.

Abstract

Aspergillus candidus is a species frequently isolated from stored grain, food, indoor environment, soil and occasionally also from clinical material. Recent bioprospecting studies highlighted the potential of using *A. candidus* and its relatives in various industrial sectors as a result of their significant production of enzymes and bioactive compounds. A high genetic variability was observed among *A. candidus* isolates originating from various European countries and the USA, that were mostly isolated from indoor environments, caves and clinical material. The *A. candidus sensu lato* isolates were characterized by DNA sequencing of four genetic loci, and agreement between molecular species delimitation results, morphological characters and exometabolite spectra were studied. Classical phylogenetic methods (Maximum likelihood, Bayesian inference) and species delimitation methods based on the multispecies coalescent model supported recognition of up to three species in *A. candidus sensu lato*. After evaluation of phenotypic data, a broader species concept was adopted, and only one new species, *A. dobrogensis*, was proposed. This species is represented by 22 strains originating from seven countries (ex-type strain CCF 4651^{T} = NRRL 62821^{T} = IBT 32697^{T} = CBS 143370^{T}) and its differentiation from *A. candidus* is relevant for bioprospecting studies because these species produce different exometabolite profiles. Evaluation of the antifungal susceptibility of sect. *Candidi* members to six antifungals using the reference EUCAST method showed that all species have low minimum inhibitory concentrations for all tested antifungals. These results suggest applicability of a wide spectrum of antifungal agents for treatment of infections caused by species from sect. *Candidi*.

Introduction

Aspergillus section *Candidi* [1] currently encompasses six white- or yellow-sporulating species [2-4]. Apart from their morphology, which is broadly uniform across the majority of species, the taxonomy of the section is based on the physiology, exometabolite profiles and molecular data [2, 3]. *Aspergillus candidus* is the best known member of sect. *Candidi*. It is a xerophile and commonly found on stored grain, where it can decrease the grains' germinability. It is also frequently encountered in the indoor environment, on stored food and feedstuff (seeds, spices, grain products, nuts, dried products) and in soil [5-10].

Aspergillus candidus produces many bioactive compounds including anti-oxidative [11-14], cytotoxic [15], antitumor [16] and antimicrobial [11, 17, 18]. The species also has the potential to be used in biotechnology and waste degradation, as a result of its significant production of extracellular enzymes (e.g. acetamidase, inulinase, lipase, xylanase, etc.) [19-24] or in food manufacturing processes [25-28]. A variety of superficial and invasive infections have been attributed to *A. candidus* [29]; however, at least some of these cases were presumably caused by a related species *A. tritici* [2, 30, 31].

A considerable genetic variability was observed among *A. candidus* isolates during our previous studies on cave and indoor mycobiota and clinical fungi. In order to substantiate the initial finding, we assembled *A. candidus* strains isolated from various substrates in different European countries and the USA. We conducted DNA sequencing of four genetic loci, classical phylogenetic analysis, coalescence analysis, analysis of morphology and exometabolite spectra, and physiological testing in order to elucidate whether the detected level of genetic variability reflects undescribed species diversity or a high infraspecific variability.

Materials and Methods

Molecular studies. DNA was extracted from seven-day-old colonies with the ArchivePure DNA yeast and Gram2+ kit (5PRIME Inc., Gaithersburg, Maryland) using modifications described by Hubka *et al.* [32]. The ITS rDNA region was amplified using forward primers ITS1 and ITS5 [33] and reverse primers ITS4S [34] or NL4 [35]; partial *benA* gene encoding β-tubulin using forward primers Bt2a [36] or Ben2f [37] and reverse primer Bt2b [36]; partial *CaM* gene encoding calmodulin using forward primers CF1M or CF1L and reverse primer CF4 [38]; partial *RPB2* gene using forward primers fRPB2-5F [39] or RPB2-F50-CanAre [40] and reverse primer fRPB2-7cR [39]. The PCR protocol was described by Hubka *et al.* [2]. *RPB2* gene fragments were amplified using standard or touchdown thermal cycling [41].

PCR product purification followed the protocol described by Réblová *et al.* [42]. Automated sequencing was performed at Macrogen Sequencing Service (Amsterdam, The Netherlands) using the forward and reverse primers. Sequences were inspected and assembled using Bioedit v. 7.1.8 (www.mbio.ncsu.edu/BioEdit/bioedit.html). Obtained DNA sequences were deposited into the ENA (European Nucleotide Archive) database (Table 1).

Phylogenetic analysis. The ITS rDNA region was not used for phylogenetic analysis due to its low number of informative positions as recognized previously [2-4]. Alignments of the *benA*, *CaM* and *RPB2* regions were performed using the G-INS-i option implemented in [43]. Alignments were trimmed, concatenated and then analysed using Maximum Likelihood (ML) and Bayesian Inference (BI) analyses. The alignments is available from the Dryad Digital Repository: https://doi.org/10.5061/dryad.pg143.

A suitable partitioning scheme and substitution models (Bayesian information criterion) for analyses were selected using greedy strategy implemented in PartitionFinder v1.1.1 [44] with settings allowing introns, exons and codon positions to be independent partitions. The optimal partitioning scheme for ML analysis divided the dataset into five partitions with the following substitution models: K80+G substitution model was proposed for the *benA* and *CaM* introns; HKY+G model for the 3rd codon positions of *benA* and *CaM*; TrN+I model for 1st codon positions of *RPB2*, *benA* and *CaM*; HKY model for 2nd codon positions of *RPB2 benA* and *CaM*; and HKY+G model for the 3rd codon positions of *RPB2*. The ML tree was constructed with IQ-TREE version 1.4.4 [45] with nodal support determined by non-parametric bootstrapping (BS) with 1000 replicates. *Aspergillus petersonii* CCF 4999 was used as an outgroup.

Bayesian posterior probabilities (PP) were calculated using MrBayes 3.2.6 [46]. The optimal partitioning scheme and substitution models were selected as described above. The optimal partitioning scheme for BI analysis was similar to that for ML analysis except for the GTR+I model proposed for the 1st codon positions of *RPB2*, *benA* and *CaM*. The analyses ran for 10^7 generations, two parallel runs with four chains each were used, every 1000th tree was retained, and the first 25 % of trees were discarded as burn-in. Convergence was assessed by examining the likelihood plots in Tracer v. 1.6 [47].

Species delimitation using methods based on the multispecies coalescent model (MSC) and species tree inference. Three single-locus species delimitation methods, i.e., bGMYC [48], GMYC [49] and mPTP [50], and one multi locus species delimitation method STACEY [51] were used to find putative species boundaries within isolates identified as *A. candidus*. We followed Carstens *et al.* [52] and compared the results of several different methods. Three

genetic loci (*benA*, *CaM* and *RPB2*) were analyzed. Nucleotide substitution models for particular loci were determined using jModeltest v. 2.1.7 [53] based on Bayesian information criterion (BIC) and were as follows: K80 (*benA*), TrNef+I (*CaM*), TrN+I (*RPB2*).

Single locus ultrametric trees were constructed using a Bayesian approach in BEAST v. 2.4.5 [54] with both Yule and coalescent tree models. These trees were used as an input for the bGMYC and GMYC methods. Chain length for each tree was 1×10^7 generations with 25 % burn-in. The highest credibility tree was used for the GMYC method and 100 trees randomly sampled throughout the analysis were used for the bGMYC method. Both methods were performed in R 3.3.4 [55] using *bgmyc* [48] and *splits* (SPecies' LImits by Threshold Statistics) [49] packages. The non-ultrametric trees for the mPTP method were constructed using the ML approach in RAxML v. 7.7.1 [56] and IQ-TREE v. 1.5.3 [45] with 1000 bootstrap replicates. The mPTP programme was used with the following setting: Maximum likelihood species delimitation inference (option ML) and a different coalescent rate for each delimited species (option multi).

The multilocus species delimitation was performed in BEAST v. 2.4.5 with add-on STACEY v. 1.2.2 [51]. The chain length was set to 5×10^8 generations, priors were set as follows: the species tree prior was set to the Yule model, growth rate prior was set to lognormal distribution (M = 5, S = 2), clock rate priors for all loci were set to lognormal distribution (M = 0, S = 1), PopPriorScale prior was set to lognormal distribution (M = -7, S = 2) and relativeDeathRate prior was set to beta distribution ($\alpha = 1$, $\beta = 1000$). The output was processed with SpeciesDelimitationAnalyzer [51]. We also tested possible influence of strict and relaxed clock models on the results, but we did not find any differences.

The species tree was inferred using *BEAST [57] implemented in BEAST v. 2.4.5. For this analysis, only unique combined nucleotide sequences were selected with DAMBE v. 6.4.11 [58]. The isolates were assigned to a putative species according to the results of the above-mentioned species delimitation methods. The MCMC analysis ran for 1×10^8 generations, 25 % of trees were discarded as a burn-in. The strict molecular clock was chosen for all loci and population function was set as constant. Convergence was assessed by examining the likelihood plots in Tracer v. 1.6 [47]. We also constructed the tree with the same settings as above, but with each isolate defined as separate species.

The validation of the species hypotheses was performed in BP&P v. 3.3 (Bayesian phylogenetics and phylogeography) [59]. The isolates were assigned to the species based on the results of species delimitation methods and the species tree inferred with *BEAST was used as a guide tree. Three different combinations of the prior distributions of the parameters

θ (ancestral population size) and τ_0 (root age) were tested as proposed by Leaché and Fujita (2010), i.e., large ancestral population sizes and deep divergence: θ ~ G (1, 10) and τ_0 ~ G (1, 10); small ancestral population sizes and shallow divergences among species: θ ~ G (2, 2000) and τ_0 ~ G (2, 2000); large ancestral populations sizes and shallow divergences among species: θ ~ G (1, 10) and τ_0 ~ G (2, 2000).

R package *ggtree* [60] and the programme Densitree [61] were used for visualization of the phylogenetic trees.

Phenotypic studies and statistical analysis. For macormorphological characterization, the strains were grown on malt extract agar (MEA; malt extract from Oxoid Ltd., Basingstoke, UK), Czapek Yeast Extract Agar (CYA; yeast extract from Oxoid Ltd.), Czapek-Dox Agar (CZA) and Czapek Yeast Extract Agar with 20 % sucrose (CY20S). Agar media composition was based on that described by Samson *et al.* [62]. The production of acid compounds into the agar medium was tested on creatine sucrose agar (CREA). Growth at 30, 33, 35 and 37 °C was tested on MEA. Colour determination was performed according to the ISCC-NBS Centroid Colour Charts [63] (http://tx4.us/nbs-iscc.htm).

The micromorphology was observed on MEA after 10–14d of incubation at 25 °C as described by Hubka *et al.* [64]. Morphological characters were recorded at least 35 times for each isolate. Statistical differences in particular characters between species were tested with one-way ANOVA followed by Tukey´s HSD (honest significant difference) test in R v. 3.3.4 [55]. R package *multcomp* [65] was used for the calculation and package *ggplot2* [66] for visualization of the results.

Exometabolite analysis. The extracts were prepared according to Houbraken *et al.* [67]. Fungi were incubated for 1 week at 25 °C in darkness on CYA and yeast extract sucrose (YES) agars for exometabolite analysis. High-performance liquid chromatography with diode-array detection was performed according to Frisvad and Thrane [68, 69] as updated by Nielsen *et al.* [70].

Antifungal susceptibility testing. The determination of the minimum inhibitory concentrations (MICs) of antifungal agents was carried out according to the reference European Committee on Antimicrobial Susceptibility testing (EUCAST) guidelines (E.Def 9.3) for amphotericin B, terbinafine, itraconazole, posaconazole, voriconazole and isavuconazole [71]. Manufacturers and stock solutions (5000 mg L^{-1}) in DMSO (dimethyl sulfoxide; Sigma-Aldrich, Vallensbæk Strand, Denmark) were as follows: terbinafine (Novartis, Basel, Switzerland), posaconazole (Merck, Sharp and Dohme, Glostrup, Denmark), amphotericin B and itraconazole (Sigma-Aldrich, Brøndby, Denmark), isavuconazole

(Astellas Pharma Inc, Tokyo, Japan) and voriconazole (Pfizer A/S, Ballerup, Denmark). Plates were incubated at 30 °C to promote growth as suggested in EUCAST E.Def 7.2. *Candida parapsilosis* ATCC 22019 and *Candida krusei* ATCC 6258 were included as quality controls.

Results

Phylogenetic analysis

In the phylogenetic analysis, 54 combined *benA*, *CaM* and *RPB2* sequences were assessed for members of sect. *Candidi* (isolation source and accession numbers are listed in Table 1). The concatenated alignment contained 2133 characters, with 537 variable and 262 parsimony informative sites. In the best scoring Maximum likelihood tree shown in Fig. 1, members of sect. *Candidi* are resolved in several monophyletic clades or isolated single-strain lineages corresponding to six currently recognized species, namely *A. candidus*, *A. campestris*, *A. subalbidus*, *A. taichungensis*, *A. pragensis* and *A. tritici*. Twenty-one *Aspergillus* isolates originating from Romanian caves (n=11), indoor environment (n=6), clinical material (n=2) and mouse and herbivore dung (n=2) formed a highly supported monophyletic lineage (ML bootstrap support 91 % and BI posterior probability 0.99) sister to *A. candidus* s. str. These strains differed from *A. candidus* by phenotypic characters (see below) and are described below as *A. dobrogensis*.

The isolates of *A. dobrogensis* clustered into two highly supported clades, while several weakly supported clades were present in the *A. candidus* lineage (Fig. 1). Eleven of twenty *A. dobrogensis* isolates were recovered from the cave environment of three Romanian caves, where this species was most frequently found on bat guano (Fig. 2) and in the cave sediment. Further strains were obtained from indoor environment, clinical material and dung evidencing that *A. dobrogensis* is not exclusively a troglobitic species. Clade 1 of *A. dobrogensis* lineage (Fig. 1) contained only isolates from caves (n=9), while clade 2 (n=12) contained mostly isolates from the indoor environment (indoor air, carpet, dust, surface of a museum piece) and clinical material (human nails), but also two strains from caves and two strains from dung.

The ITS rDNA sequences of all investigated *A. dobrogensis* strains were identical to *A. candidus*, *A. subalbidus* and *A. pragensis*. The *benA* sequence of the ex-type strain of *A. dobrogensis* CCF 4651^{T} showed 95.3 % similarity to the ex-type of *A. candidus* NRRL 303^{T} (444/466 bp). The similarity of the *CaM* and *RPB2* sequences to *A. candidus* NRRL 303^{T} are 98.2 % (557/567 bp) and 98.6 % (1000/1014 bp), respectively. The infraspecific genetic varibility between *A. dobrogensis* strains was low making it easily distinguishable from *A.*

candidus by using *benA*, *CaM* and *RPB2* loci. There were seven variable sites in the *benA* alignment, eight in the *RPB2* alignment and only one in *CaM* alignment.

Species delimitation using MSC-based methods

Three genetic loci were examined across isolates identified as *A. candidus sensu lato*; and *A. tritici* lineage was also included in the analysis. Three tentative species (*A. tritici, A. candidus* and *A. dobrogensis*) were delimited in the analyzed dataset using the multi-locus delimitation method STACEY. The results are summarised in Fig. 3, and the differences in the colour of the tree branches reflect the proposed species delimitation.

Aspergillus tritici was consistently delimited from *A. candidus* and *A. dobrogensis* by all single-locus methods including their different settings (Fig. 3). Various delimitation schemes were proposed by different single-locus species delimitation methods in the *A. candidus*/*A. dobrogensis* lineages. The mPTP method based on all three loci and also bGMYC analysis based on the *RPB2* locus (only with input tree constructed using coalescent tree model) did not support delimitation of *A. dobrogensis* from *A. candidus*. In contrast, the results of bGMYC method based on the *benA* (input tree constructed using coalescent tree model), *CaM* and *RPB2* datasets (input tree constructed using Yule tree model) were in full agreement with the results of the STACEY analysis (Fig. 3). The GMYC method based on the *benA* and *RPB2* locus and also the bGMYC method based on *benA* locus (input tree constructed using Yule tree model) supported delimitation of an additional species within the *A. dobrogensis* lineage, corresponding to the two highly supported clades observed in the BI and ML analysis (Fig. 1). A significant over delimitation was observed in *A. candidus*/*A. dobrogensis* lineages when analyzing the *CaM* locus by GMYC method. The GMYC method also delimited several additional species in *A. candidus* lineage when analyzing *benA* and *RPB2* loci (Fig. 3). These putative species gained no support by any other analyses.

The species validation analysis results are appended to nodes of the tree in Fig. 3. Delimitation of all putative species proposed by STACEY were supported by the posterior probability 1.00 based on the analysis in BP&P v. 3.1 [59] under all three scenarios simulated by different prior distributions of parameters θ (ancestral population size) and τ_0 (root age).

The species tree topology was inferred with *BEAST [57] and is shown in Fig. 4. The analysis supported existence of up to four species that were highly supported (posterior probabilities = 1.00), i.e., *A. tritici*, *A. candidus* s. str. and two putative species in the *A. dobrogensis* lineage. There was no evidence of recombination between members of these lineages.

Phenotypic analysis

Growth parameters and macromorphological characters were assessed on four media and five temperatures. The results are summarized in Table 2. The colony morphology and growth parameters of *A. dobrogensis* are similar to those of *A. candidus*; however, on average, *A. dobrogensis* grows faster at 25 °C on all tested media (Table 2). The length and width of the stipe, and the diameter of vesicles significantly differed (Tukey´s HSD test, p value < 0.001) between *A. candidus* and *A. dobrogensis* (Fig. 5). The length of stipe was the most useful feature for differentiation of these species due to relatively lower overlap of values. The diameter of the conidia was identical for both species (Table 2, Fig. 5). No significant phenotypic differences were observed between isolates representing the two *A. dobrogensis* subclades (data not shown).

Exometabolites

There are chemotaxonomical differences between *A. candidus* and *A. dobrogensis* (Table 3). Barceloneic acid C, candidusins, terphenyllin and aspergilazine A are only found in some *A. candidus* isolates. A broad profile of aspergiloids [72] are found in *A. dobrogensis*, while only one aspergiloid is found in some strains of *A. candidus*. Brevianamide F seems to be a precursor of 12,13-dehydrodesoxybrevianamide E [= prolyl-2-(1',1'-dimethylallyl)tryptophyldiketopiperazine] and related compounds previously found in *A. pseudoustus* and *Pencillium italicum* [73-75]. They are found in both species, but *A. dobrogensis* produces a broader spectrum of these compounds. Similarly, the "Paspa" compounds are found in both species, but again *A. dobrogensis* produce a more broad profile of these compounds. These compounds may be equal to okaramins S-U [76], but this has yet to be confirmed. The uncharacterized compounds "ALKO", "MOYN", "MYO" and "TUT" are only found in *A. candidus*, while the "FMI" and the red compounds "AQ RED1" and "AQ RED2" are only found in *A. dobrogensis*. Retention indices and UV absorption maxima for the detected extrolites in *A. candidus* and *A. dobrogensis* are summarized in Table S1.

Antifungal susceptibility testing according the EUCAST method

The minimum inhibitory concentration (MIC) ranges and geometric mean (GM) values obtained by the EUCAST reference method for six antifungal agents (terbinafine, posaconazole, isavuconazole, voriconazole, itraconazole, amphotericin B) are shown in Table 4. Overall, all isolates across species in sect. *Candidi* were as susceptible as *A. fumigatus* to the

azoles and amphotericin B as MICs were below the EUCAST epidemiologic cut off values for these compounds against *A. fumigatus* (itraconazole: 1 mg/L, posaconazole: 0.25 mg/L, voriconazole: 1 mg/L, isavuconazole: 2 mg/L and amphotericin B: 1 mg/L) (Arendrup *et al.*, 2012; Arendrup *et al.*, 2016; Hope *et al.*, 2013). Exceptions were one isolates of *A. subalbidus* and one isolates of *A. taichungensis* for which the MIC of voriconazole was one dilution above the *A. fumigatus* ECOFF. Elevated MICs to terbinafine (4 mg L^{-1}) were recorded for two isolates of *A. candidus* and one isolate of *A. subalbidus*.

Description of *Aspergillus dobrogensis* A. Nováková, Ž. Jurjević, F. Sklenar, Frisvad, Houbraken & Hubka, sp. nov. (Figs. 2, 6)

Aspergillus dobrogensis (do.bro.gen´sis. N.L. masc. adj. *dobrogensis* pertaining to Dobrogea, Romania, the region of origin of the type specimen).

Description of micromorphology. *Conidial heads* on MEA white to cream white, radiate, biseriate, arising from aerial hyphae, rope-like structures occasionally present, coiling hyphae occasionally present. *Stipes* hyaline, smooth-walled, occasionally finely roughened, occasionally septate, (125–)150–2200(–3000) × (3.5–)4–13(–15) µm, diminutive conidiophores common, up to 100 long × 3–4(–5) µm diam; *vesicles* globose to subglobose, occasionally pyriform to elongate, (8–)9–31(–36) µm diam, diminutive vesicles 4–9 µm diam; *metulae* wedge-shaped (V-shaped) to cylindrical, (3–)4–17(–36) × (3–)4–10(–16) µm, covering the entire surface of vesicle; *phialides* ampuliform, (5–)6–9(–12) × 2.5–3.5(–4) µm, occasionally solitary phialides present up to 17 µm long. *Conidia* globose to subglobose, (3–)3.5–5(–5.5) µm (4 ± 0.3 µm), occasionally broadly ellipsoidal, smooth walled, occasionally finely roughened, larger spores borne on large phialides**.** *Sclerotia* purplish to black, occasionally cream to brown, sparse to abundant on MEA and CYA after 8 weeks.

Culture characteristics (at 25 °C after 2 wk). Colonies on MEA (21−)30−34(−37) mm diam (13−22 mm in 7 d), plane to delicately furrowed, zonate, delicately granular to granular, sporulation on whole surface or only in the colony centre with submerged margins, yellowish white (ISCC−NBS No. 92), no exudate, no soluble pigment, reverse colourless. Colonies on CYA (30−)38−42(−46) mm diam (18−26 mm in 7 d), plane to irregularly furrowed, with submerged margin, velutinous to delicately granular, sometimes floccose in colony centre, white (No. 263) to yellowish white (No. 92), no exudate to very small colourless droplets, no

soluble pigment, reverse colourless. Colonies on CZA (21−)24−28(−33) mm diam (12−17 mm in 7 d), plane, submerged lobate margins, zonate, delicately granular, yellowish white (No. 92), no exudate, no soluble pigment, reverse colourless. After 30 d the reverse is dark grey (No. 266) with occasional production of a dark grey soluble pigment. Colonies on CY20S (32−)35−38(−48) mm diam (20−27 mm in 7 d), plane with umbonate centre, floccose to delicately granular or granular, yellowish white (No. 92) to pale greyish yellow (No. 90) in colony centre, no exudate, no soluble pigment, reverse colourless to moderate yellow (No. 87). Growth parameters on MEA at 30 °C are comparable to 25 °C, no strains grew at 35 °C (Table 2).

The holotype specimen, PRM 935751, is deposited in the herbarium of the Mycological Department, National Museum, Prague, Czech Republic (PRM), and was isolated from cave sediment in the Movile Cave (Airbell II), Dobrogea region, Romania, collected and isolated by A. Nováková. The culture ex type is CCF 4651^{T} (= CCF 4655^{T} = NRRL 62821^{T} = IBT 32697^{T} = CBS 143370^{T}). The MycoBank deposit number is MB821313.

Morphological comparisons. *Aspergillus dobrogensis* differs from *A. candidus* by its longer and broader stipes and statistically significantly smaller vesicles (Table 2, Fig. 5). Almost all isolates of *A. dobrogensis* produced sclerotia on MEA and CYA, while the majority of *A. candidus* strains examined in this study did not produce sclerotia on CYA and none of the isolates produced them on MEA. In general, the average growth of *A. dobrogensis* isolates at 25 °C was more rapid on all tested media compared to *A. candidus* (Table 2). *Aspergillus campestris* can be differentiated by its sulfur yellow colonies; growth parameters of *A. pragensis* are slower on all media (especially CZA) and temperatures, and the colony reverse on MEA turns to red-brown after 2–3 weeks of cultivation; *A. subalbidus* grows also slightly slower than *A. dobrogensis* and has shorter stipes on MEA; *A. tritici* and *A. taichungensis* can be differentiated by their ability to grow at 37 °C.

Substrate and distribution. The species is known from bat droppings and guano, cave sediment, cave air, indoor air, dust, carpet, mouse dung, herbivore dung and clinical material; Czech Republic, Denmark, Germany, Romania, the Netherlands, Spain and the USA.

Discussion

A high degree of genetic variability among isolates of *A. candidus* was previously reported by Varga *et al.* [3], who preferred a broad species concept for *A. candidus*. As we demonstrated in this study, genetic diversity of *A. candidus sensu lato* strains is underlayed by both infraspecific variability and undescribed species diversity. The delimitation of a new species, *A. dobrogensis*, from *A. candidus* was supported by a polyphasic approach comprising multilocus sequence analyses, morphological and exometabolite data. Despite a relatively strong ecological clustering of the *A. dobrogensis* isolates into two clades with also high statistical phylogenetic support (Fig. 1), phenotypic or extrolite differences supporting the delimitation of two species in the *A. dobrogensis* lineage were not found. Due to this, we decided to introduce only one species, *A. dobrogensis*. In general, the ecology of *A. candidus* is very similar to *A. dobrogensis* and both species occur sympatrically on similar substrates (Fig. 1, Table 1).

Members of sect. *Candidi* are infrequently implicated in human infections. Although few in number, a wide spectrum of infections have been attributed to *A. candidus*, including invasive aspergillosis [77], lung abscess [78], meningitis [79], granuloma of the brain [80], sinusitis [81], otitis externa [2, 82-86] and onychomycosis [87-94]. Another member of sect. *Candidi*, *A. tritici*, is probably responsible for a part of reported infections attributed to *A. candidus* because it is able to grow at 37 °C in contrast to *A. candidus*. This species revived by Varga *et al.* [3] has been repeatedly detected in clinical samples when molecular methods were employed for species identification [30, 31, 95], and it has been confirmed as an agent of onychomycosis [30, 95]. In addition, some unrelated species can be misidentified as members of sect. *Candidi*. For instance, well-known causal agents of aspergillosis such as *A. fumigatus*, *A. flavus* and *A. terreus* occasionally produce white spored mutants [3, 96-98] and some naturally white spored species from sect. *Terrei* (*A. carneus* and *A. niveus*) are able to cause human infections as well [2, 99-102]. *Aspergillus pragensis*, a recently described member of sect. *Candidi* based on two isolates from clinical material in the Czech Republic, was isolated from indoor environment and outdoor air in the USA during this study (Fig. 1, Table 1) and was recently reported from Canadian house dust [10]. Clinical relevance of this species remains unconfirmed because both cases of suspected onychomycosis were not supported by repeated isolation of the species as required by guidelines for diagnosis of non-dermatophyte onychomycosis [103].

Previous studies reported a high *in vitro* activity of common antifungal agents against *A. candidus* [2, 104-106] and *A. tritici* [2, 31]. However, these studies usually included a limited number of isolates, used different methodologies for susceptibility testing and the characterization of strains was often based on phenotypic characters, resulting in unreliable

identifications. High MICs to amphotericin B detected in several isolates identified as *A. candidus* [105, 107] may indicate misidentification with species from sect. *Terrei* that are typical by intrinsic resistance to this antifungal [108]. In general, our results confirmed good *in vitro* activity of six antifungal agents against all members of sect. *Candidi* (Table 4). There was no clear antifungal susceptibility pattern typical for a particular species and overall the susceptibility pattern was similar to that for *A. fumigatus* [71, 109, 110].

Earlier studies on exometabolite production by members of sect. *Candidi* showed that these species produce unique compounds chlorflavonins, terphenyllin and candidusins, that are not present in other aspergilli [2, 3, 12, 111], except for *A. ellipticus* from sect. *Nigri* [112]. All these compounds have anti-oxidative properties, and they are most likely overproduced to protect the white/yellow conidia rather than via melanin, as opposed to species in closely related section *Nigri* that produce very large amounts of melanins [111].

Interestingly, antioxidant compounds candidusins, terphenyllin and its derivate 3-hydroxyterphenyllin were only detected in some strains of *A. candidus* while chlorflavonin was present in all examined strains of *A. candidus* and *A. dobrogensis* (Table 3). Thus, differentiation of these two species seems to be relevant especially for bioprospecting studies. For instance, antioxidant activity of some compounds and no production of mycotoxins make *A. candidus* suitable for the use in fermentation industry [28], and the extrolite 3-hydroxyterphenyllin has promising anticancer activity [16]. Similarly, barceloneic acid C, a compound with antibacterial activity [113] and aspergilazine A [114], which has antiviral activity, were detected only in *A. candidus* strains and not in *A. dobrogensis*. The production of many other uncharacterized compounds with unknown activity is in some cases species-specific (Table 3). It can be expected that both species also differ in extracellular enzymes production, some of which have industrial potential [19-24].

Funding Information

This research was supported by Czech Science Foundation (grant No. 17-20286S) and the project BIOCEV (CZ.1.05/1.1.00/02.0109) provided by the Ministry of Education, Youth and Sports of CR and ERDF. Vit Hubka is grateful for support from the Czechoslovak Microscopy Society (CSMS scholarship 2016).

Acknowledgements

We thank Milada Chudíčková and Birgit Brandt for her invaluable assistance in the laboratory, Stephen W. Peterson and P. Lysková for providing some isolates and the CCF

collection staff (Alena Kubátová - curator, Ivana Kelnarová and Adéla Kovaříčková) for deposition and lyophilization of the majority of cultures, and Veronica Jurjević for editing. Vit Hubka is grateful for support from Czechoslovak Microscopy Society (CSMS scholarship 2016).

Conflicts of Interest

The authors declare that that there is no conflict of interest.

References

1. Gams W, Christensen M, Onions AH, Pitt JI, Samson RA. Infrageneric taxa of *Aspergillus*. In: Samson RA, Pitt JI, editors. Advances in *Penicillium* and *Aspergillus* Systematics. New York: Plenum Press; 1985. p. 55–62.

2. Hubka V, Lyskova P, Frisvad JC, Peterson SW, Skorepova M, Kolarik M. *Aspergillus pragensis* sp. nov. discovered during molecular re-identification of clinical isolates belonging to *Aspergillus* section *Candidi*. Med Mycol. 2014;52:565–76.

3. Varga J, Frisvad JC, Samson RA. Polyphasic taxonomy of *Aspergillus* section *Candidi* based on molecular, morphological and physiological data. Stud Mycol. 2007;59:75–88.

4. Visagie CM, Hirooka Y, Tanney JB, Whitfield E, Mwange K, Meijer M, et al. *Aspergillus*, *Penicillium* and *Talaromyces* isolated from house dust samples collected around the world. Stud Mycol. 2014;78:63–139.

5. Klich MA. Biogeography of *Aspergillus* species in soil and litter. Mycologia. 2002;94(1):21–7.

6. Papavizas G, Christensen C. Grain storage studies. XXIX. Effect of invasion by individual species and mixtures of species of *Aspergillus* upon germination and development of discolored germs in wheat. Cereal Chem. 1960;37(2):197–203.

7. Pitt JI, Hocking AD. *Aspergillus* and related teleomorphs. In: Pitt JI, Hocking AD, editors. Fungi and food spoilage. London: Springer; 2009. p. 275-337.

8. Samson RA, Houbraken J, Thrane U, Frisvad JC, Andersen B. Food and indoor fungi. Utrecht: CBS KNAW Biodiversity Center; 2010. 269 p.

9. Sinha R, Wallace H. Storage stability of farm-stored rapeseed and barley. Can J Plant Sci. 1977;57(2):351–65.

10. Visagie CM, Yilmaz N, Renaud JB, Sumarah MW, Hubka V, Frisvad JC, et al. A survey of xerophilic *Aspergillus* from indoor environment, including descriptions of two new section *Aspergillus* species producing eurotium-like sexual states. MycoKeys. 2017;19:1–30.

11. Elaasser MM, Abdel-Aziz MM, El-Kassas RA. Antioxidant, antimicrobial, antiviral and antitumor activities of pyranone derivative obtained from *Aspergillus candidus*. Journal of Microbiology and Biotechnology Research. 2017;1(4):5–17.
12. Rahbæk L, Frisvad JC, Christophersen C. An amendment of *Aspergillus* section *Candidi* based on chemotaxonomical evidence. Phytochemistry. 2000;53(5):581–6.
13. Yen G-C, Chang Y-C, Sheu F, Chiang H-C. Isolation and characterization of antioxidant compounds from *Aspergillus candidus* broth filtrate. J Agric Food Chem. 2001;49(3):1426-31.
14. Yen G-C, Chiang H-C, Wu C-H, Yeh C-T. The protective effects of *Aspergillus candidus* metabolites against hydrogen peroxide-induced oxidative damage to Int 407 cells. Food Chem Toxicol. 2003;41(11):1561–7.
15. Takahashi C, Yoshihira K, Natori S, Umeda M. The structures of toxic metabolites of *Aspergillus candidus*. I. The compounds A and E, cytotoxic p-terphenyls. Chem Pharm Bull. 1976;24(4):613–20.
16. Wang Y, Compton C, Rankin GO, Cutler SJ, Rojanasakul Y, Tu Y, et al. 3-Hydroxyterphenyllin, a natural fungal metabolite, induces apoptosis and S phase arrest in human ovarian carcinoma cells. Int J Oncol. 2017;50(4):1392–402.
17. Shemshura ON, Bekmakhanova NE, Mazunina MN, Meyer SL, Rice CP, Masler EP. Isolation and identification of nematode-antagonistic compounds from the fungus *Aspergillus candidus*. FEMS Microbiol Lett. 2016;363(5):fnw026.
18. Wang R, Guo ZK, Li XM, Chen FX, Zhan XF, Shen MH. Spiculisporic acid analogues of the marine-derived fungus, *Aspergillus candidus* strain HDf2, and their antibacterial activity. Antonie Leeuwenhoek. 2015;108(1):215–9.
19. Farias CM, de Souza OC, Sousa MA, Cruz R, Magalhães OMC, de Medeiros ÉV, et al. High-level lipase production by *Aspergillus candidus* URM 5611 under solid state fermentation (SSF) using waste from *Siagrus coronata* (Martius) Becari. Afr J Biotechnol. 2015;14(9):820–8.
20. Garai D, Kumar V. Response surface optimization for xylanase with high volumetric productivity by indigenous alkali tolerant *Aspergillus candidus* under submerged cultivation. 3 Biotech. 2013;3(2):127–36.
21. Kochhar A, Gupta AK, Kaur N. Purification and immobilisation of inulinase from *Aspergillus candidus* for producing fructose. J Sci Food Agric. 1999;79(4):549–54.
22. Milala M, Shehu B, Zanna H, Omosioda V. Degradation of agro-waste by cellulase from *Aspergillus candidus*. Asian Journal of Biotechnology. 2009;1(2):51–6.

23. Rahim M, Saxena R, Gupta R, Sheoran A, Giri B. A novel and quick plate assay for acetamidase producers and process optimization for its production by *Aspergillus candidus*. Process Biochemistry. 2003;38(6):861–6.
24. Zheng P, Yu H, Sun Z, Ni Y, Zhang W, Fan Y, et al. Production of galacto-oligosaccharides by immobilized recombinant β- galactosidase from *Aspergillus candidus*. Biotechnol J. 2006;1(12):1464–70.
25. Grazia L, Romano P, Bagni A, Roggiani D, Guglielmi G. The role of moulds in the ripening process of salami. Food Microbiol. 1986;3(1):19–25.
26. Spotti E, Mutti P, Scalari F. *Penicillium nalgiovense*, *P. gladioli*, *P. candidum* and *Aspergillus candidus*. Possibility of their use as starter cultures. Industria Conserve. 1994;69:237–41.
27. Sunesen L, Stahnke L. Mould starter cultures for dry sausages—selection, application and effects. Meat Sci. 2003;65(3):935–48.
28. Yen GC, Chang YC, Su SW. Antioxidant activity and active compounds of rice koji fermented with *Aspergillus candidus*. Food Chem. 2003;83(1):49–54.
29. de Hoog GS, Guarro J, Gené J, Figueras MJ. Atlas of Clinical Fungi, 4th. ed. (USB-version). Utrecht: CBS-KNAW Fungal Biodiversity Centre; 2014.
30. Hubka V, Kubatova A, Mallatova N, Sedlacek P, Melichar J, Skorepova M, et al. Rare and new aetiological agents revealed among 178 clinical *Aspergillus* strains obtained from Czech patients and characterised by molecular sequencing. Med Mycol. 2012;50:601–10.
31. Masih A, Singh PK, Kathuria S, Agarwal K, Meis JF, Chowdhary A. Clinically significant rare *Aspergillus* species in a referral chest hospital, Delhi, India: molecular and MALDI TOF identification and their antifungal susceptibility profiles. J Clin Microbiol. 2017:doi:10.1128/JCM.00962-16
32. Hubka V, Kolařík M, Kubátová A, Peterson SW. Taxonomical revision of *Eurotium* and transfer of species to *Aspergillus*. Mycologia. 2013;105:912–37.
33. White TJ, Bruns T, Lee S, Taylor J. Amplification and direct sequencing of fungal ribosomal RNA genes for phylogenetics. In: Innis MA, Gelfand DH, J. SJ, White TJ, editors. PCR protocols: a guide to methods and applications. San Diego: Academic Press; 1990. p. 315–22.
34. Kretzer A, Li Y, Szaro T, Bruns TD. Internal transcribed spacer sequences from 38 recognized species of *Suillus* sensu lato: phylogenetic and taxonomic implications. Mycologia. 1996;88(5):776–85.

35. O'Donnell K. *Fusarium* and its near relatives. In: Reynolds DR, Taylor JW, editors. The Fungal Holomorph: Mitotic, Meiotic and Pleomorphic Speciation in Fungal Systematics Wallingford: CAB International; 1993. p. 225–33.
36. Glass NL, Donaldson GC. Development of primer sets designed for use with the PCR to amplify conserved genes from filamentous ascomycetes. Appl Environ Microbiol. 1995;61(4):1323–30.
37. Hubka V, Kolařík M. β-tubulin paralogue *tubC* is frequently misidentified as the *benA* gene in *Aspergillus* section *Nigri* taxonomy: primer specificity testing and taxonomic consequences. Persoonia. 2012;29:1–10.
38. Peterson SW. Phylogenetic analysis of *Aspergillus* species using DNA sequences from four loci. Mycologia. 2008;100(2):205–26.
39. Liu YJ, Whelen S, Hall BD. Phylogenetic relationships among ascomycetes: evidence from an RNA polymerse II subunit. Mol Biol Evol. 1999;16(12):1799–808.
40. Jurjević Ž, Kubátová A, Kolařík M, Hubka V. Taxonomy of *Aspergillus* section *Petersonii* sect. nov. encompassing indoor and soil-borne species with predominant tropical distribution. Pl Syst Evol. 2015;301:2441–62.
41. Hubka V, Nováková A, Peterson SW, Frisvad JC, Sklenář F, Matsuzawa T, et al. A reappraisal of *Aspergillus* section *Nidulantes* with descriptions of two new sterigmatocystin producing species. Pl Syst Evol. 2016;302:1267–99.
42. Réblová M, Hubka V, Thureborn O, Lundberg J, Sallstedt T, Wedin M, et al. From the tunnels into the treetops: new lineages of black yeasts from biofilm in the Stockholm metro system and their relatives among ant-associated fungi in the *Chaetothyriales*. PLoS One. 2016;11(10):e0163396.
43. Katoh K, Standley DM. MAFFT multiple sequence alignment software version 7: improvements in performance and usability. Mol Biol Evol. 2013;30(4):772–80.
44. Lanfear R, Calcott B, Ho SY, Guindon S. PartitionFinder: combined selection of partitioning schemes and substitution models for phylogenetic analyses. Mol Biol Evol. 2012;29(6):1695–701.
45. Nguyen L-T, Schmidt HA, von Haeseler A, Minh BQ. IQ-TREE: A fast and effective stochastic algorithm for estimating maximum-likelihood phylogenies. Mol Biol Evol. 2015;32(1):268–74.
46. Ronquist F, Teslenko M, van der Mark P, Ayres DL, Darling A, Höhna S, et al. MrBayes 3.2: efficient Bayesian phylogenetic inference and model choice across a large model space. Syst Biol. 2012;61:539-42.

47. Rambaut A, Suchard M, Xie D, Drummond A. Tracer v1. 6. 2014, website http://beast.bio.ed.ac.uk 2014.
48. Reid NM, Carstens BC. Phylogenetic estimation error can decrease the accuracy of species delimitation: a Bayesian implementation of the general mixed Yule-coalescent model. BMC Evol Biol. 2012;12(1):196.
49. Fujisawa T, Barraclough TG. Delimiting species using single-locus data and the Generalized Mixed Yule Coalescent approach: a revised method and evaluation on simulated data sets. Syst Biol. 2013;62(5):707–24.
50. Kapli P, Lutteropp S, Zhang J, Kobert K, Pavlidis P, Stamatakis A, et al. Multi-rate Poisson tree processes for single-locus species delimitation under maximum likelihood and Markov chain Monte Carlo. Bioinformatics. 2017;33(11):1630–8.
51. Jones G. Algorithmic improvements to species delimitation and phylogeny estimation under the multispecies coalescent. J Math Biol. 2017;74(1-2):447–67.
52. Carstens BC, Pelletier TA, Reid NM, Satler JD. How to fail at species delimitation. Mol Ecol. 2013;22(17):4369–83.
53. Posada D. jModelTest: phylogenetic model averaging. Mol Biol Evol. 2008;25(7):1253–6.
54. Bouckaert R, Heled J, Kühnert D, Vaughan T, Wu C-H, Xie D, et al. BEAST 2: a software platform for Bayesian evolutionary analysis. PLoS Comput Biol. 2014;10(4):e1003537.
55. R_Core_Team. R: A language and environment for statistical computing. Vienna: R Foundation for Statistical Computing; 2015.
56. Stamatakis A, Hoover P, Rougemont J. A rapid bootstrap algorithm for the RAxML web servers. Syst Biol. 2008;57(5):758–71.
57. Heled J, Drummond AJ. Bayesian inference of species trees from multilocus data. Mol Biol Evol. 2010;27(3):570–80.
58. Xia X. DAMBE6: new tools for microbial genomics, phylogenetics, and molecular evolution. J Hered. 2017;108(4):431–7.
59. Yang Z, Rannala B. Bayesian species delimitation using multilocus sequence data. Proceedings of the National Academy of Sciences. 2010;107(20):9264–9.
60. Yu G, Smith DK, Zhu H, Guan Y, Lam TTY. ggtree: an R package for visualization and annotation of phylogenetic trees with their covariates and other associated data. Methods Ecol Evol. 2017;8(1):28–36.

61. Bouckaert RR. DensiTree: making sense of sets of phylogenetic trees. Bioinformatics. 2010;26(10):1372–3.
62. Samson RA, Visagie CM, Houbraken J, Hong SB, Hubka V, Klaassen CHV, et al. Phylogeny, identification and nomenclature of the genus *Aspergillus*. Stud Mycol. 2014;78:141–73.
63. Kelly KL. Inter-society color council – National bureau of standards color name charts illustrated with centroid colors. Washington: US Government Printing Office; 1964. 36 p.
64. Hubka V, Novakova A, Kolarik M, Jurjevic Z, Peterson SW. Revision of *Aspergillus* section *Flavipedes*: seven new species and proposal of section *Jani* sect. nov. Mycologia. 2015;107(1):169–208.
65. Hothorn T, Bretz F, Westfall P. Simultaneous inference in general parametric models. Biometrical Journal. 2008;50(3):346–63.
66. Wickham H. ggplot2: Elegant Graphics for Data Analysis. New York: Springer-Verlag; 2009.
67. Houbraken J, Spierenburg H, Frisvad JC. *Rasamsonia*, a new genus comprising thermotolerant and thermophilic *Talaromyces* and *Geosmithia* species. Antonie Leeuwenhoek. 2012;101(2):403–21.
68. Frisvad JC, Thrane U. Standardized high-performance liquid chromatography of 182 mycotoxins and other fungal metabolites based on alkylphenone retention indices and UV-VIS spectra (diode array detection). J Chromatogr A. 1987;404(1):195–214.
69. Frisvad JC, Thrane U. Liquid column chromatography of mycotoxins. In: Betina V, editor. Chromatography of mycotoxins: techniques and applications Journal of Chromatography Library 541993. p. 253–372.
70. Nielsen KF, Månsson M, Rank C, Frisvad JC, Larsen TO. Dereplication of microbial natural products by LC-DAD-TOFMS. J Nat Prod. 2011;74(11):2338–48.
71. Arendrup MC, Meletiadis J, Mouton J, Guinea J, Cuenca-Estrella M, Lagrou K, et al. EUCAST technical note on isavuconazole breakpoints for *Aspergillus*, itraconazole breakpoints for *Candida* and updates for the antifungal susceptibility testing method documents. Clin Microbiol Infect. 2016;22(6):571. e1-. e4.
72. Guo ZK, Yan T, Guo Y, Song YC, Jiao RH, Tan RX, et al. P-terphenyl and diterpenoid metabolites from endophytic *Aspergillus* sp. YXf3. J Nat Prod. 2012;75(1):15–21.
73. Arai K, Miyajima H, Mushiroda T, Yamamoto Y. Metabolites of *Penicillium italicum* Wehmer: isolation and structures of new metabolites including naturally occurring 4-ylidene-

acyltetronic acids, italicinic acid and italicic acid. Chemical and Pharmaceutical Bulletin. 1989;37(12):3229–35.

74. Steyn P. Austamide, a new toxic metabolite from *Aspergillus ustus*. Tetrahedron Lett. 1971;12(36):3331–4.

75. Steyn P. The structures of five diketopiperazines from *Aspergillus ustus*. Tetrahedron. 1973;29(1):107–20.

76. Cai S, Sun S, Peng J, Kong X, Zhou H, Zhu T, et al. Okaramines S–U, three new indole diketopiperazine alkaloids from *Aspergillus taichungensis* ZHN-7-07. Tetrahedron. 2015;71(22):3715–9.

77. Iwasaki K, Tategami T, Sakamoto Y, Yasutake T, Otsubo S. An operated case report of pulmonary aspergillosis by sapprophytic infection of Aspergillus candidus in congenital bronchial cyst of right lower lobe. Kyobu geka The Japanese journal of thoracic surgery. 1991;44(5):429-32.

78. Becker A, Sifaoui F, Gagneux M, Desprez S, Vignoli P, Huguet D, et al. Drug interactions between voriconazole, darunavir/ritonavir and tenofovir/emtricitabine in an HIV-infected patient treated for *Aspergillus candidus* lung abscess. Int J STD AIDS. 2015;26(9):672–5.

79. Moling O, Lass- Floerl C, Verweij P, Porte M, Boiron P, Prugger M, et al. Chronic and acute *Aspergillus* meningitis. Mycoses. 2002;45(11–12):504–11.

80. Linares G, McGarry PA, Baker RD. Solid solitary aspergillotic granuloma of the brain Report of a case due to *Aspergillus candidu*s and review of the literature. Neurology. 1971;21(2):177–84.

81. Avanzini F, Bigoni A, Nicoletti G. A rare case of isolated aspergilloma of the sphenoid sinus. Acta Otorhinolaryngol Ital. 1991;11(5):483–9.

82. Falser N. Mycotic infection of the ear. Harmless saprophyte or pathognomonic risk factor? PILZBEFALL DES OHRES - HARMLOSER SAPROPHYT ODER PATHOGNOMONISCHER RISIKOFAKTOR? 1983;62(4):140-6.

83. García-Agudo L, Aznar-Marín P, Galán-Sánchez F, García-Martos P, Marín-Casanova P, Rodríguez-Iglesias M. Otomycosis due to filamentous fungi. Mycopathologia. 2011;172(4):307–10.

84. Vennewald I, Schönlebe J, Klemm E. Mycological and histological investigations in humans with middle ear infections. Mycoses. 2003;46(1- 2):12-8.

85. Vennewald I, Schönlebe J, Klemm E. Histologic studies on otomycosis. Mycoses. 2002;45:47-52.

86. Yassin A, Maher A, Moawad M. Otomycosis: a survey in the eastern province of Saudi Arabia. J Laryngol Otol. 1978;92(10):869–76.
87. Ahmadi B, Hashemi SJ, Zaini F, Shidfar MR, Moazeni M, Mousavi B, et al. A case of onychomycosis caused by *Aspergillus candidus*. Med Mycol Case Rep. 2012;1(1):45–8.
88. Cornere B, Eastman M. Onychomycosis due to *Aspergillus candidus*: case report. N Z Med J. 1975;82(543):13–5.
89. Fragner P, Kubickova V. Onychomycosis due to *Aspergillus candidus*. Cesk Dermatol. 1974;49(5):322–4.
90. Gupta A, Gupta G, Jain H, Lynde C, Foley K, Daigle D, et al. The prevalence of unsuspected onychomycosis and its causative organisms in a multicentre Canadian sample of 30 000 patients visiting physicians' offices. J Eur Acad Dermatol Venereol. 2016;30(9):1567–72.
91. Kaben U. *Aspergillus candidus* Link as the cause of onychomycosis. Z Haut Geschlechtskr. 1962;32:50–3.
92. Nouripour-Sisakht S, Mirhendi H, Shidfar M, Ahmadi B, Rezaei-Matehkolaei A, Geramishoar M, et al. *Aspergillus* species as emerging causative agents of onychomycosis. J Mycol Med. 2015;25(2):101–7.
93. Piraccini BM, Tosti A. White superficial onychomycosis: epidemiological, clinical, and pathological study of 79 patients. Arch Dermatol. 2004;140(6):696–701.
94. Zaror L, Moreno M. Onychomycosis due to *Aspergillus candidus* Link. Rev Argent Micol. 1980;3(3):13–5.
95. Zotti M, Machetti M, Persi A, Barabino G, Mariotti M, Parodi A. Different species of *Aspergillus* involved in ungual pathologies. Journal of Biological Research-Bollettino della Società Italiana di Biologia Sperimentale. 2011;84(1):171–3.
96. Cole RJ, Hill RA, Blankenship PD, Sanders TH. Color mutants of *Aspergillus flavus* and *Aspergillus parasiticus* in a study of preharvest invasion of peanuts. Appl Environ Microbiol. 1986;52(5):1128–31.
97. Jackson JC, Higgins LA, Lin X. Conidiation color mutants of *Aspergillus fumigatus* are highly pathogenic to the heterologous insect host *Galleria mellonella*. PLoS One. 2009;4(1):e4224.
98. Raper KB, Fennell DI. The genus *Aspergillus*. Baltimore: Williams & Wilkins Co.; 1965. 686 p.

99. Auberger J, Lass-Flörl C, Clausen J, Bellmann R, Buzina W, Gastl G, et al. First case of breakthrough pulmonary *Aspergillus niveus* infection in a patient after allogeneic hematopoietic stem cell transplantation. Diagn Microbiol Infect Dis. 2008;62(3):336–9.
100. Morquer R, Enjalbert L. Sur un nouvel agent de l'aspergillose humaine. Rev Mycol Paris. 1957;22:130–54.
101. Morquer R, Enjalbert L. Étude morphologique et physiologique d'une *Aspergillus* nouvellement isolé au cors d'un affection pulmonaire de l'homme. C R Soc Biol Paris. 1957;244:1405–8.
102. Pore R, Larsh H. Experimental pathology of *Aspergillus terreus-flavipes* group species. Med Mycol. 1968;6(2):89–93.
103. Summerbell RC, Cooper E, Bun U, Jamieson F, Gupta AK. Onychomycosis: A critical study of techniques and criteria for confirming the etiologic significance of nondermatophytes. Med Mycol. 2005;43(1):39–59.
104. García-Martos P, García-Agudo L, Gutiérrez-Calzada J, Ruiz-Aragón J, Saldarreaga A, Marín P. In vitro activity of amphotericin B, itraconazole and voriconazole against 20 species of *Aspergillus* using the Sensititre® microdilution method. Enferm Infecc Microbiol Clin. 2005;23(1):15–8.
105. Gomez-Lopez A, Garcia-Effron G, Mellado E, Monzon A, Rodriguez-Tudela JL, Cuenca-Estrella M. In vitro activities of three licensed antifungal agents against Spanish clinical isolates of *Aspergillus* spp. Antimicrob Agents Chemother. 2003;47(10):3085–8.
106. Wildfeuer A, Seidl H, Paule I, Haberreiter A. *In vitro* evaluation of voriconazole against clinical isolates of yeasts, moulds and dermatophytes in comparison with itraconazole, ketoconazole, amphotericin B and griseofulvin. Mycoses. 1998;41(7- 8):309–19.
107. Dóczi I, Dósa E, Varga J, Antal Z, Kredics L, Nagy E. Etest for assessing the susceptibility of filamentous fungi. Acta Microbiol Immunol Hung. 2004;51(3):271–81.
108. Risslegger B, Zoran T, Lackner M, Aigner M, Sánchez-Reus F, Rezusta A, et al. A prospective international *Aspergillus terreus* survey: an EFISG, ISHAM and ECMM joint study. Clin Microbiol Infect. 2017:doi:10.1016/j.cmi.2017.04.012.
109. Arendrup MC, Cuenca- Estrella M, Lass- Flörl C, Hope W. EUCAST technical note on the EUCAST definitive document EDef 7.2: method for the determination of broth dilution minimum inhibitory concentrations of antifungal agents for yeasts EDef 7.2 (EUCAST-AFST). Clin Microbiol Infect. 2012;18(7):E246–E7.

110. Hope W, Cuenca- Estrella M, Lass- Flörl C, Arendrup M, (EUCAST-AFST) TECoASTSoAST. EUCAST technical note on voriconazole and *Aspergillus* spp. Clin Microbiol Infect. 2013;19(6):E278–E80.
111. Frisvad JC, Larsen TO. Chemodiversity in the genus *Aspergillus*. Appl Microbiol Biotechnol. 2015;99(19):7859–77.
112. Samson RA, Noonim P, Meijer M, Houbraken J, Frisvad JC, Varga J. Diagnostic tools to identify black aspergilli. Stud Mycol. 2007;59:129–45.
113. Xia X, Kim S, Bang S, Lee H-J, Liu C, Park C-I, et al. Barceloneic acid C, a new polyketide from an endophytic fungus *Phoma* sp. JS752 and its antibacterial activities. J Antibiot. 2015;68(2):139–41.
114. Cai S, Kong X, Wang W, Zhou H, Zhu T, Li D, et al. Aspergilazine A, a diketopiperazine dimer with a rare N-1 to C-6 linkage, from a marine-derived fungus *Aspergillus taichungensis*. Tetrahedron Lett. 2012;53(21):2615–7.

Figure legends

Fig. 1. Phylogenetic relationships of the sect. *Candidi* members inferred from Bayesian analysis of the combined, 3-gene data set of β-tubulin (*benA*), calmodulin (*CaM*) and RNA polymerase II second largest subunit (*RPB2*) genes. Bayesian posterior probability (PP) and Maximum likelihood bootstrap support (BS) are appended to nodes; only PP ≥ 90 % and BS ≥ 70 % and are shown; lower supports are indicated with a hyphen; ex-type strains are designated by a superscript T. The tree is rooted with *Aspergillus petersonii* CCF 4999^{T}.

Fig. 2. Colonies of *Aspergillus dobrogensis* on bat guano in the Liliecilor de la Gura Dobrogei Cave (a–b).

Fig. 3. Schematic representation of results of species delimitation methods in section *Candidi* based on *benA*, *CaM* and *RPB2* sequence data. The results of multilocus method (STACEY) are compared to results of single-locus methods. The results of STACEY are shown as tree branches with different colours, while the results of single-locus methods (PTP, bGMYC, GMYC) are depicted with coloured bars (different colours, including different colour shades, indicate tentative species delimited by particular methods). The species validation analysis results (BP&P) are appended to nodes and shown in gray bordered boxes; the values represent posterior probabilities calculated in three scenarios [top value: $\theta \sim G(1, 10)$ and $\tau_0 \sim G(1,$

10); middle value: θ ~ G (1, 10) and τ_0 ~ G (2, 2000); bottom value: θ ~ G (2, 2000) and τ_0 ~ G (2, 2000)]. The displayed maximum likelihood tree was inferred with IQ-TREE and based on a concatenated alignment of *benA*, *CaM* and *RPB2* loci [1000 bootstrap replicates; partitioning scheme was determined as described in Material and Methods], and is used solely for the comprehensive presentation of the results from different methods.

Fig. 4. Species tree inferred with *BEAST visualized by using DensiTree (Bouckaert 2010). All trees created in the analysis (except 25 % burn-in phase) are displayed, the consensus trees is highlighted by blue-coloured line. The MCMC analysis ran for 1×10^8 generations, 25 % of trees were discarded as a burn-in. The strict molecular clock was chosen for all loci and population function was set as constant. Convergence was assessed by examining the likelihood plots in Tracer v. 1.6 (Rambaut *et al.,* 2014). Bayesian posterior probability (PP) are appended to nodes; only PP ≥ 90 % are shown. The isolates were assigned to a putative species according to the consensual results of the species delimitation methods, i.e, *A. tritici*, *A. candidus*, and two putative species in *A. dobrogensis* lineage (a). Alternativelly, each isolate having unique haplotype was defined as separate species (b).

Fig. 5. Differences between selected phenotypic characters of *Aspergillus candidus* (n=12) and *A. dobrogensis* (n=12). The length and the width of the stipe, and also vesicle diameter were significantly different (Tukey´s HSD test, p value < 0.001) between species, in contrast to diameter of conidia. Boxplots show median, interquartile range, values within ± 1.5 of interquartile range (whiskers) and outliers. Boxplots and violin graphs were created in R 3.3.4 (R Core Team 2015) with package *ggplot2* (Wickham 2009).

Fig. 6. Macromorphology and micromorphology of *Aspergillus dobrogensis*. (a–d) Colonies on MEA, CYA, CZA and CY20S (from the right to left) incubated 14 d at 25 °C. (e–h) Biseriate conidiophores. (i) Conidia. (j) Sclerotia. Bar = 10 µm (e–i).